

Wave added resistance implementation in a routing software

A performance prediction optimization
for Wind-Assisted Cargo Ships

Graduation Thesis M.Sc. Marine Technology
Martin Fonbonne



Wave added resistance implementation in a routing software

A performance prediction optimization
for Wind-Assisted Cargo Ships

by

Martin Fonbonne

Performed at

VPLP Design

to obtain the degree of Master of Science in Marine Technology in the specialization of ship design
at the Delft University of Technology,

to be defended publicly on Monday November 18th, 2024 at 2 PM.

Student number: 5722462
Project duration: December 1, 2023 – September 30, 2024

Company supervisors: Thomas Abikhzir, VPLP Design
Xavier Guisnel, VPLP Design

Supervisor: Ir. J.Gelling, TU Delft
Thesis committee: Prof. G. Weymouth, TU Delft
Dr. AA Kana, TU Delft

This thesis (MT.24/25.013.M) is classified as confidential in accordance with the general conditions for projects performed by the TUDelft

Cover: Canopée, Tom Van Oossanen



Acknowledgements

This report is a reflection of work during my graduation thesis in order to obtain my Master of Science degree in Marine Technology at Delft University of Technology. Most of the work presented in this report was done at VPLP Design.

First of all, I would like to thank my supervisor, Ir. Jaap Gelling who was always available to answer my questions. His help and advice played a great role in the success of this thesis which would not have been possible without him.

I would also like to thank Simon Watin and Xavier Guisnel from VPLP Design for accepting me in their company and for helping me during the time I spent there. Furthermore, I especially thank Thomas Abikhzir for his help, patience, knowledge, and for answering all my questions even the most ridiculous ones! I spent a great time in this company and learnt a lot thanks to them.

Eventually, I would also like to thank my parents for their unconditional support during this thesis and more generally during my whole studies. They provided me with the best in life and I could never be more grateful. Furthermore, I would like to thank Cassandre for being there for me at all times.

This report also marks the end of my studies in Delft. I also thank my colleagues and friends for all the memorable moments during this journey.

Martin Fonbonne
Paris, France
September 2024

Summary

In the context of global warming, all sectors must rapidly decrease their dependence on fossil fuels in order to cut down their CO₂ emissions. Naturally, the maritime sector is no exception and is actively looking for carbon free alternatives. Among the different technologies developed to achieve this goal, the Wind Assisted Ship Propulsion is quite promising as it could cut down a ship's fuel consumption by up to 30%.

VPLP design aims to develop such technology. However in the performance prediction phase, the company needs to be able to assess the wave added resistance. The scientific literature has provided us with a good knowledge of this resistance and some semi-empirical methods to evaluate it. Yet, these models can be quite different and it is important to test which one is the most efficient for a RoRo ship depending on the case study. A python package has been made to compute it easily depending on simple ship parameters and sea conditions. Furthermore, four methods are included in the program and the latter can choose which one is best adapted depending on the case study.

Another challenge with wind assisted propulsion is the need for an adapted routing system. It needs to be able to find the best route to optimize the use of sails and thus reduce the fuel consumption. As an input, it requires a polar matrix with fuel consumption depending on the wind conditions and the ship's speed. The wave added resistance can have a large impact on fuel consumption (around 20% more than only calm water resistance) therefore, it was implemented and added. The program now takes 6D polar matrices which also include the significant wave height, the wave length and the wave angle. It enables to have a more realistic and relevant routing system. Furthermore, a study on routing software's space step was conducted to find its influence on the results.

Eventually, the company often needs to perform statistical weather studies. These studies can improve the performance prediction loop by showing the most frequent weather conditions and their impact on a ship or a ship's journey. It can be used to implement the wave added resistance or even for engine/propeller matching. The study usually use data from the last years. However, the polar matrices can be quite large with many improbable cases which ought to be optimized. A program was coded to retrieve wave data and perform studies on the different sea conditions a ship could encounter over a journey. One can now check for the most frequent wind/wave combinations and adjust the design or the VPP loop.

Eventually, some of the limits of this project are mentioned. First of all, the wave added resistance program requires to be validated more thoroughly and it is planned to be compared with future onboard data. Furthermore, many steps in the routing software or within the statistical study tools have a large computational time. Some solutions are suggested but there is still room for improvement. Eventually, some files are getting particularly large and programs struggle to handle it. A judicious choice in the number of data could help reduce the sizes of some documents.

Overall, the tasks were completed and the new programs are currently being used by the company. Although validation measures and improvements must be done, this thesis can help companies to improve sailing cargo ships' VPP. With the right routing software, wind assisted propulsion can be used to their full potential and help reduce the shipping industry's carbon footprint.

Contents

Acknowledgements	i
Summary	ii
Nomenclature	v
1 Introduction	1
1.1 Global Context Presentation	1
1.1.1 Maritime industry CO2 emissions and environmental impact	1
1.1.2 Sailing assistance to reduce CO2 emissions	1
1.1.3 Challenges regarding Wind-assisted ship propulsion	3
1.2 Company Presentation: VPLP Design	4
1.2.1 General overview of the company	4
1.2.2 Maritime pole and projects	5
1.2.3 Need for routing optimization	6
1.3 Research goal and project	6
1.3.1 Problem definition	6
1.3.2 Routing software	7
1.3.3 Wave added resistance: how to model and implement it	7
1.3.4 Tool for statistical studies	8
1.3.5 Scope of the project	8
1.3.6 Report structure	8
2 Wave added Resistance	10
2.1 Literature review	10
2.1.1 Theoretical background	10
2.1.2 Numerical and experimental resolution	13
2.1.3 Semi empirical methods	16
2.1.4 State of the art and scope for this thesis	17
2.2 Importance of quantification for performance prediction	17
2.2.1 Influence on fuel consumption	17
2.2.2 Criteria of selection	18
2.3 Appropriate models for the project	19
2.3.1 First and second model: Liu and Papanikolaou (2021) and Mittendorf et al. (2023)	19
2.3.2 Third model: Lang and Mao (2021)	22
2.3.3 Fourth model: Kim and Kim (2022)	23
2.3.4 Program verification and methodology	24
2.4 Implementation of the wave added resistance for VPLP Design	27
2.4.1 Irregular waves calculation	27
2.4.2 Implementation for VPLP Design's needs: PyWave package	29
2.4.3 Results and comparisons	34
2.4.4 Limits and suggestions	38
3 Routing software optimization	39
3.1 Software Presentation	39
3.1.1 TZStat routing software	39
3.1.2 Specific use for VPLP Design	40
3.2 Influence of space step	41
3.2.1 Method for assessing the influence of space step	41
3.2.2 Impact on computational time	44

4	Optimized tool for metoceanic analysis	45
4.1	Depiction of statistical analysis	45
4.1.1	Ships performance prediction	45
4.1.2	Particularities for WASP	46
4.1.3	From 3D to 6D study	46
4.2	Metoceanic tool for a specific journey	47
4.2.1	PyRoute package optimization	47
4.2.2	From a route to desired wind/wave components	47
4.2.3	Examples and results	48
4.2.4	Suggestions for improvement	50
5	Conclusion	52
5.1	Final tool	52
5.1.1	Wave added resistance implementation	52
5.1.2	Routing software optimization	52
5.1.3	Statistical analysis program	53
5.1.4	Tool combination for an overall performance prediction	53
5.2	Main project conclusions	53
5.2.1	Results and Discussion	53
5.2.2	Limits	54
5.2.3	Suggestions for further improvements	54
	References	56

Nomenclature

Abbreviations

Abbreviation	Definition
ECMWF	European Centre for Medium-Range Weather Forecasts
HFO	Heavy Fuel Oil
IMO	International Maritime Organisation
ITTC	International Towing Tank Conference
JONSWAP	Joint North Sea Wave Observation Project
LNG	Liquefied Natural Gas
MSE	Mean squared error
VPP	Velocity prediction program
WASP	Wind Assisted Ship Propulsion

Symbols

Symbol	Definition	Unit
a_1	amplitude factor	\square
a_2	speed correction factor	\square
B	beam	[m]
B_f	bluntness coefficient factor	\square
C_{AW}	non dimensional wave added resistance	\square
C_b	Block coefficient	\square
C_{H_s}	wave height correction factor	\square
d	depth	[m]
E	average entrance angle	[°]
F_r	Froude number	\square
g	gravitational constant	[m/s ²]
H_s	significant wave height	[m]
k	wave number	[m ⁻¹]
k_{yy}	non dimensional radius of gyration	\square
l_e	length of entrance	[m]
L_{pp}	length between perpendiculars	[m]
l_r	length of run	[m]
P_b	Propulsive power	[W]
R_{AW}	wave added resistance	[N]
R_{AWM}	ship motion component of R_{AW}	[N]
R_{AWR}	diffraction effect component of R_{AW}	[N]
$R_{T,calm}$	calm water resistance	[N]
R_{wind}	wind resistance	[N]
STW	speed through water	[m/s]
t	regular wave period	[s]
T	draft	[m]

Symbol	Definition	Unit
T_a	aft draft	[m]
T_f	forward draft	[m]
T_m	mean period	[s]
T_{max}	maximum draft	[m]
T_p	peak period	[s]
T_z	zero-crossing period	[s]
TWA	true wind angle	[°]
TWS	true wind speed	[m/s]
V or U	ship speed	[m/s]
V_c	Phase velocity	[m/s]
V_g	Group velocity	[m/s]
α	wave angle	[°]
α_T	draft coefficient	[]
γ	JONSWAP enhancement factor	[]
ζ	wave amplitude	[m]
η_D	propulsive efficiency	[]
η_M	transmission efficiency	[]
θ	waterline segment inclination angle	[°]
λ	wavelength	[m]
ρ	density	[kg/m ³]
ω_0	incident wave frequency	[s ⁻¹]
$\bar{\omega}$	frequency factor	[]

1

Introduction

1.1. Global Context Presentation

1.1.1. Maritime industry CO₂ emissions and environmental impact

The shipping industry is responsible for around 3% of the world greenhouse gas emissions [13]. Furthermore, it is also responsible for SO_x emissions which are toxic for humans and the environment and cause acid rains. Eventually, NO_x emissions are also an important aspect of the impact of the shipping industry on the environment as it is a strong greenhouse gas and it is also toxic [42]. In order to comply with the 2015 Paris agreement, the IMO intends to drop the GHG emissions of the sector by 50% in 2050. So far, the Energy Efficiency Design Index (EEDI, 2013) sets a limit of efficiency for CO₂ emissions. On top of that, the Carbon Intensity Index (CII, 2023) will determine a carbon efficiency for each ship and will become more and more strict so as to push ship owners to invest for the most sustainable options.

Furthermore, on a local scale, the noise made by the ships and especially by the engines and the propellers' cavitation is known for harming the underwater biodiversity with serious consequences [6].

In order to reduce the CO₂, NO_x and SO_x emissions of ships, companies involved in this sector have looked at multiple solutions. Alternative fuels are currently being developed and implemented such as LNG (liquefied natural gas) or ammonia. Another option could be the use of hydrogen or battery cells in some cases. In the case of this thesis, the focus was put on wind assistance.

1.1.2. Sailing assistance to reduce CO₂ emissions

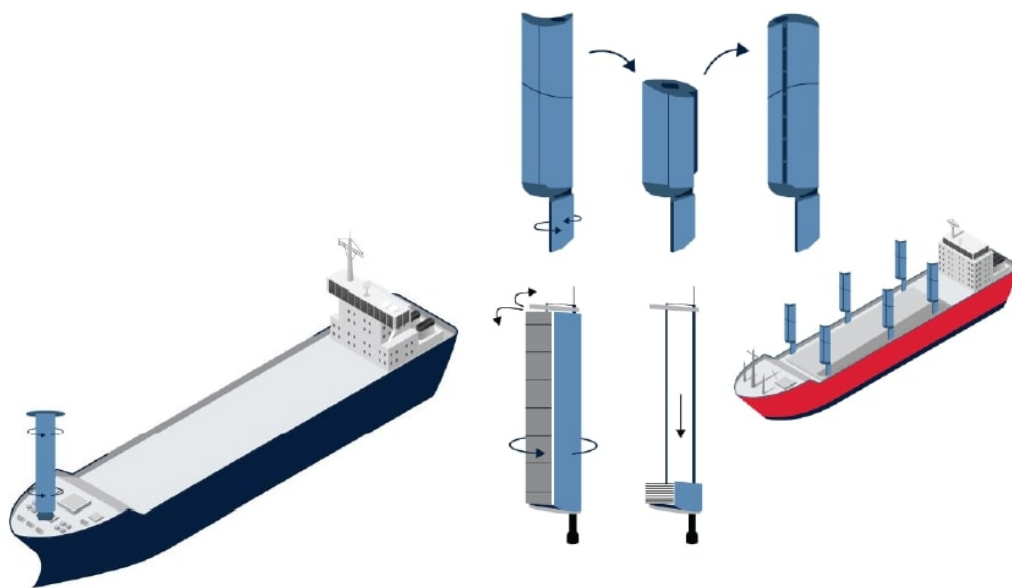
WASP or wind-assisted ship propulsion is one of the solutions proposed to reduce the GHG emissions. As the name suggests, it consists in using the power of the wind to assist or replace the engine while sailing [5]. Wind propulsion was discovered around 5000 years ago with invention of soft sails. It has then been the main power used to propel ships besides human force and enabled men to travel around the world and develop commercial routes all around the globe. In the end of the 19th century and the beginning of the 20th century, sails were progressively replaced by coal and oil engines as the resources were cheap, abundant and accessible. Moreover, these technologies were not dependant of the weather. Research then focused on improving the efficiency of propellers and engines and sailing ships were then only used for yachting and racing. However in the 1970's, the two oil crisis showed how the oil supply chain could be affected by geopolitical events and WASP regained an interest for the industry. Some prototypes of Flettner rotors were installed on ships in the 1980's but with the return

of stable oil prices, these projects were abandoned as there were considered not economically viable. Since the beginning of the 21st century, climate change and its consequences became a growing concern and the shipping industry is now looking again at alternatives for the conventional heavy fuel oil (HFO). In this context, the benefits of wind propulsion are multiple:

The wind is a free, completely renewable, abundant and inexhaustible source of energy. If coupled with an engine, it can help reduce the fuel consumption and also the noise as the latter could run with less power than usual for a fixed speed.

So far, there are different technologies used to harness the wind's power:

- One of the most common one is the implementation of Flettner rotors which use the Magnus' effect to generate thrust. They require an external source of energy to generate the rotation of the device.
- Another solution is to use hard sails or wings to generate thrust. This technology will be studied in the context of this thesis. They do not need another source of energy but are usually pilotable and their angle of attack can be modified to optimize the thrust.
- Suction wings are similar but the low pressure side sucks the air in to increase the pressure difference and thus the lift. They require an external source of energy.
- Kite sails are also in development and have the benefits catching higher and more regular winds while also not taking too much room on the deck. The way they work is quite different than the rest and will not be treated in this report.
- Eventually, soft "old school" sails can also be used in some cases.



(a) Flettner rotor

(b) Hard sails or wings

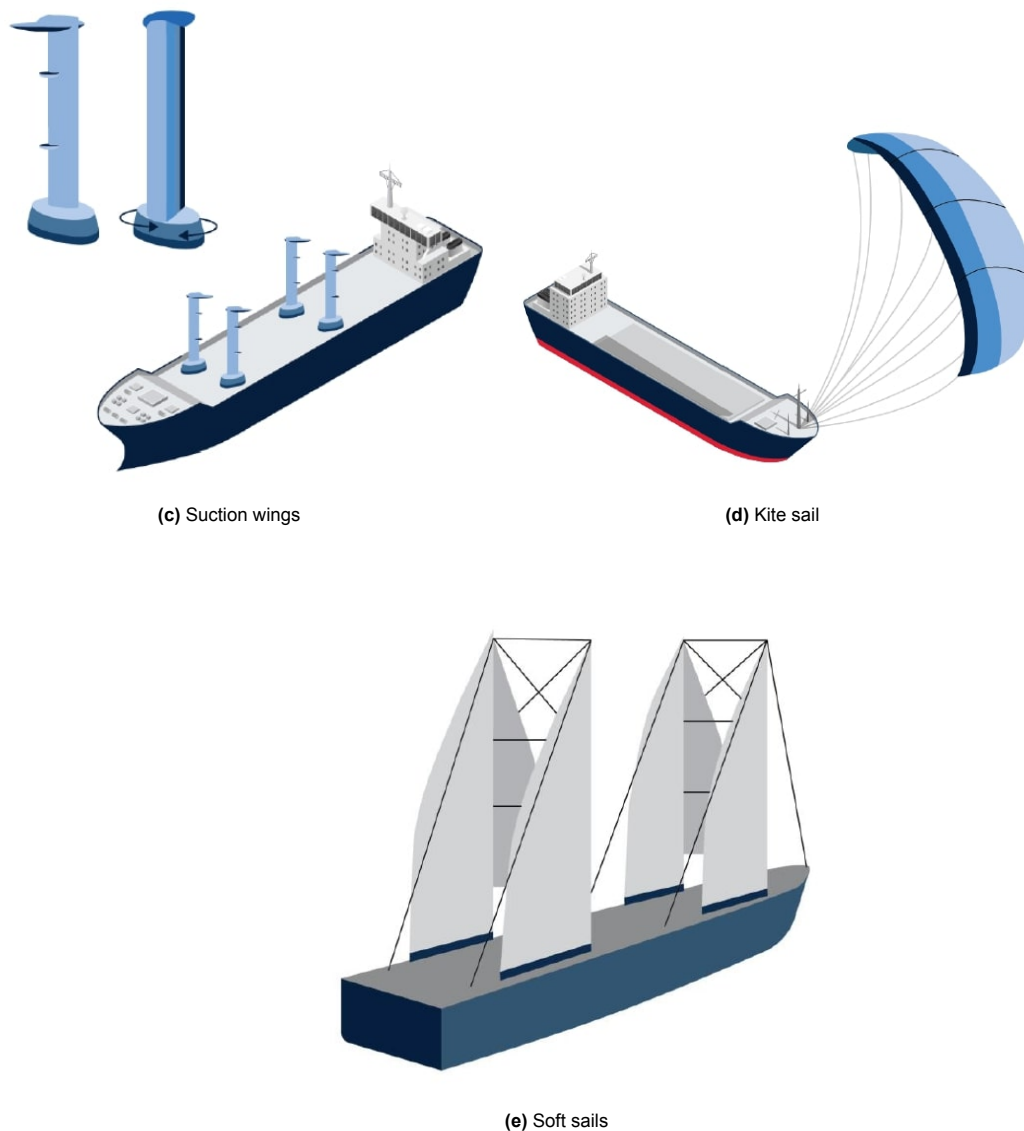


Figure 1.1: Schematics of different wind propulsion technologies

Overall, it is difficult to assess the impact on the fuel consumption and GHG reduction as it depends on a lot of different factors such as the parameters of the ship and the sails but also the on the weather conditions. It is estimated to cut down the emission of about 30% in the best case scenarios. On the other hand, some projects intend to use only the sails as a main propeller and the engine would be used only for manoeuvres at port for example. In that case, the CO₂ emissions could drop by 99%. However, the approach is totally different and it is not the case in the ships studied for this thesis.

1.1.3. Challenges regarding Wind-assisted ship propulsion

Just as any other technological solutions, WASP raises some important challenges.

Most of these technologies require room on the deck, which is not always available. In order to sail under bridges for example, it might also be important to find a way to retract the sails. The engine/propeller system needs to be able to adapt to the different thrusts delivered by the WASP system. Obviously, it raises economical questions in terms of CAPEX.

The lift generated by wings is also not exactly directed towards the direction of the ship. It tends to create a side force as well. In order to counteract this force, the hull usually acts as an opposing force by applying a certain drift angle. As a trade-off, the direction of the ship is modified and its resistance tends to increase. Due to a difference in points of application, the rudder also has to act another counter force which also generates an additional resistance. This issue raises a spark in physical research and hull improvements.

Eventually, with wind propulsion, ships are once again particularly dependent on the weather and it has a huge influence on the routing. That is why WASP systems are interesting only in parts of the world where winds are strong and regular such as trade winds for example. In order to optimize the use of the sails and minimize the fuel consumption, routing systems have become a very active field of research. This report will try to optimize the routing system in a specific case scenario which will be presented below.

1.2. Company Presentation: VPLP Design

1.2.1. General overview of the company

VPLP Design is a French-based naval architecture company founded in 1983 by Marc Van Peteghem and Vincent Lauriot-Prévost. It focuses mostly on sailing ships and became famous for the design of many racing ships who won prestigious races such as The Route du Rhum, the Vendée Globe or even the America's cup.



Figure 1.2: America's cup 2008, Oracle team USA

The company also designs yachts especially multihulls such as the Lagoon catamarans or the Gunboat catamarans. They were also involved in superyachts projects like the Douce France catamaran. Nowadays, the company has three offices, one in Paris, one in Vannes and the office in which I worked is located in Nantes, France.



Figure 1.3: Lagoon SIXTY 5

For the last decade, VPLP Design has also had projects in the maritime sector.

1.2.2. Maritime pole and projects

The company's maritime sector has developed designs for various ship types ranging from cargos to offshore service vessels or rescue vessel with a specific focus on cutting down the sector's CO2 emissions. As the company is specialized in sailing, most of their commercial ships are equipped with sails or wings. So far, one of their biggest and most famous project is Canopée, a 120m long cargo used by the European Space Agency (ESA) to carry the pieces of the next Ariane 6 rocket from European countries to Kourou in French Guiana where it is to be launched.



Figure 1.4: Canopée

These wings reduce the fuel consumption by around 15% but this reduction can go up to 30% in good conditions. However, in order to save fuel, a new challenge arises: routing optimization.

1.2.3. Need for routing optimization

A classic engine-driven ship will usually try to sail through the shortest route between two coordinates (i.e the orthodromic distance). A wing-assisted ship however, must find a route with the best meteorological conditions to optimize the use of sails [7]. As a naval architecture office, VPLP has to compute the performance of its designs. In order to provide accurate performance predictions for its customers, the company uses a routing software which takes into account the effect of the wind speed and wind angle on the fuel consumption. However, the influence of waves is not taken into account. So far, it is used only as a performance study tool for engineers and naval architects and not as an onboard routine system used by the crew for example.

1.3. Research goal and project

This research project was divided in three main goals which will be depicted in this section. Furthermore, the scope of the project will be presented. Eventually, the structure of this master thesis will be mentioned with the links between the parts of this master thesis.

1.3.1. Problem definition

The literature research focused on the development of semi-empirical methods to assess the wave added resistance and on the routing software designed for wind-assisted cargo ships. At this point, four semi-empirical models have been mostly used as they are the most convenient: they can be applied to all kind of wave directions and a large range of ships. These models have been developed with different methods and may give very different results depending on the case scenario (the wavelength, wave angle, ship type etc). That is why it is important for a potential user to know their differences and for what range these models perform best. However, there is only little research on the comparison between these different models. So far, three of them were compared however, these results have only been validated with experimental data coming from full-scale measurements of a general cargo and a container ship [62]. It could be judicious to extend this comparison for RoRo ships with a set of specific data.

When working on a performance prediction program for wind assisted ships, the wave added resistance should be added into a polar matrix: a matrix which gives the fuel consumption depending on the ship speed, the wind parameters (wind angle and wind speed) and the wave parameters (wave angle, wave height and wave period). As wind and waves are strongly correlated, it is very important to correctly assess the impact of both on a ship's fuel consumption. However, with this information, the size of polar matrices can quickly become an issue. Solutions to optimize the size of these files by focusing on the most frequent case scenario could help in reducing the size of the polar matrix and the computational time.

In view of the current literature, a clear comparison between different semi-empirical methods for wave added resistance applied to RoRo ships is missing. One should be able to find which model is the best in different case scenario. Furthermore, the optimization of polar matrices for a wind-assisted ship's performance prediction has barely been addressed.

In the context of this master's thesis, a concrete solution must be found. Therefore, the following research question can be depicted as such:

What method can be developed to choose the best wave added resistance model for a RoRo ship and how can statistical weather studies help optimize the performance prediction program of a wind-assisted ship?

This question can be divided into two parts. The first one deal with the wave added resistance, the different ways of calculating it and how to choose the best way. It can be defined with the following sub question:

How can the most accurate wave added resistance model be found depending on the conditions of the case study for a RoRo ship?

The second part deals with statistical weather studies and how they can improve the use of routing software to optimize the fuel consumption of wind-assisted ships. Especially, the wave added resistance can have a strong impact and must be taken into account in these studies. For that, a second sub question needs to be answered:

How can statistical weather studies be used to optimize the polar matrices of a performance prediction program designed for a wind-assisted ship and reduce their size?

This report will be divided in three sections to answer these questions.

1.3.2. Routing software

The routing software used by VPLP is rather new. Therefore, it was important to start by taking the hand of it. Historically, the routing used by the company is built for races across the globe and focuses on speed optimization. In the case of cargos, the optimization consists in reducing the fuel consumption and thus the greenhouse gas emissions. A first objective was to determine the influence of the space step on the accuracy and the computational time on the weather routing and the fuel consumption optimization. Here, there is a discussion in order to find the optimal space step.

The program takes a csv file with polars of the ship speed and the wind parameters and fuel consumption depending on each case scenario as an input, plus weather data and starting and arrival dates. As an output, a csv file with all the coordinates of the ship and the final consumption is generated. In this process, a second question was to figure out where and how to implement the effect of the wave added resistance.

1.3.3. Wave added resistance: how to model and implement it

The second goal was modelling the wave added resistance applied on a sailing cargo ship. This resistance would be used to calculate the ship's fuel consumption and the wave parameters would be added in polar files used by the routine software. Therefore the goal was to find an "easy" and "fast" way to implement it. Furthermore, the calculation should, if possible, only need relatively simple ship characteristics. The influence of the sails on the wave added resistance (due to leeway or yaw for example) are neglected. The proposed solution was to implement semi-empirical models as they offer a fast and quite accurate results (a further description is made below). It is important to note that semi-empirical methods are also used in other phases of the performance prediction, thus running CFD simulations on wave resistance alone would be inconsistent with the other methods. One important need was for the models to take into account the incident wave angle. In fact, most semi-empirical models only work in front wave scenarios. However, the values can be very different depending on the wave angle (adds up to 20-30% of the resistance in case of front waves but can also be negative i.e "pushes" the ship in case of following waves and relatively small ship speed [32]). Eventually, four models matched the requirements. So far, VPLP has been using one of them successfully and with a pretty good accuracy. It is explicitly detailed in an article from Mittendorf et al. [38].

Once the models are found and implemented, another question was to find a way to use the best one depending on the case scenario. Each one of them is more accurate in certain ranges depending on the ship type, the wave angle or even the wavelength ([62]). Therefore, a program must be made to determine the best model depending on the chosen case study. This program should then be validated.

Eventually, it is to be added to the overall routing software as mentioned before. It can also be used to determine the propulsion system (engine to propeller matching etc).

1.3.4. Tool for statistical studies

Finally, the company sometimes needs to perform preliminary statistical analysis of meteorological condition on a certain route. There again, the already developed tools did not take into account the wave parameters. In total, five parameters have to be studied (two from the wind: wind speed and wind direction) and three from the waves (significant wave height, wave period and wave direction). However, 5D polar files can quickly become very voluminous and thus increase the computational time. Therefore one last task was to try to optimize the statistical weather studies. One option was to decrease the size of the weather data files and focus on the most commonly encountered wind/wave parameters.

1.3.5. Scope of the project

The initial scope of the project was defined in two distinct parts.

The routing needs to be precise, with a good optimization.

The added resistance in waves has a much larger impact, and needs to be taken into account. As of today, the flat sea VPP is well suited for design studies, and has proven a good level of accuracy. This tool produces PE (Effective Power needed at the propeller) values needed to achieve a specified speed for ships equipped with WASP, presented in the form of a TWA/TWS matrix, usually called a polar matrix, or in this case a 2D/3D polar. This means 3D (Boat Speed/TWA/TWS) matrices. For the rest of the loop, an Engine Propeller Matching tool has been developed to transform the PE to PB (Brake Power) and therefore get the fuel/CO₂ consumption/emissions. To get the fuel/CO₂ consumption on a full year on a specified journey, VPLP is currently working with a third-party online software, where VPLP uploads the 3D polars and get the results a day later. The software does not handle wave added resistance, it is added later with a homemade process that needs much improvement. The purpose of this master thesis therefore follows two main objectives:

Using a local routing software that VPLP will provide, I need to develop a workflow for pre and postprocessing of route optimization runs. The ability to launch the routing software in batch (parallel computing) will be a point of focus.

Additionally, I should improve the added wave resistance treatment. This will include bibliography research, discussions on when the added waves resistance will appear in the process, integrating the wave resistance to the routing (if possible), and finally coding the wave resistance calculation. The objective is to go from 3D (BS/TWA/TWS) to 6D (Significative Wave Height H_s/ Wave Direction/ Wave period) matrices.

These two objectives were mostly fulfilled and will be detailed in this report. Moreover, during this research project more challenges arose and were dealt as well such as the influence of the space step in the routing performance predictions.

1.3.6. Report structure

After this global introduction of the context, the company and the goals of this master thesis, this report consists in a wave added resistance section which will come back on some theoretical knowledge and on the used models. Eventually, the limits and possible improvements for the wave added resistance

computation will be mentioned.

A second section deals with the routing software optimization. It will first be presented and the impact of the space step will be explained.

Eventually, the optimized tool for metoceanic analysis will be depicted and detailed with some examples.

The final section will show the results and the improvements made during this research project along with a practical explanation on how the company uses these different tools. It ends with a discussion on the limits and possible improvements of this thesis' subjects.

2

Wave added Resistance

2.1. Literature review

2.1.1. Theoretical background

Ocean waves are mechanical waves moving at the surface of the water. In the ocean, waves can be formed by different phenomena. For small periods (between 0s and 30s) waves will be formed mostly by wind blowing above the ocean. The wavelength ranges between 0m and 1km. Longer waves with a period between 30s and 5min are infra-gravity waves caused by the wind and gravity effects. Above 5min of period are the waves caused by storms or earthquakes. Eventually, waves with periods of 12 or 24h hours are tidal waves and are created by the gravitational interaction with the moon and the sun. The picture below sums up the different types of waves in the ocean [58]:

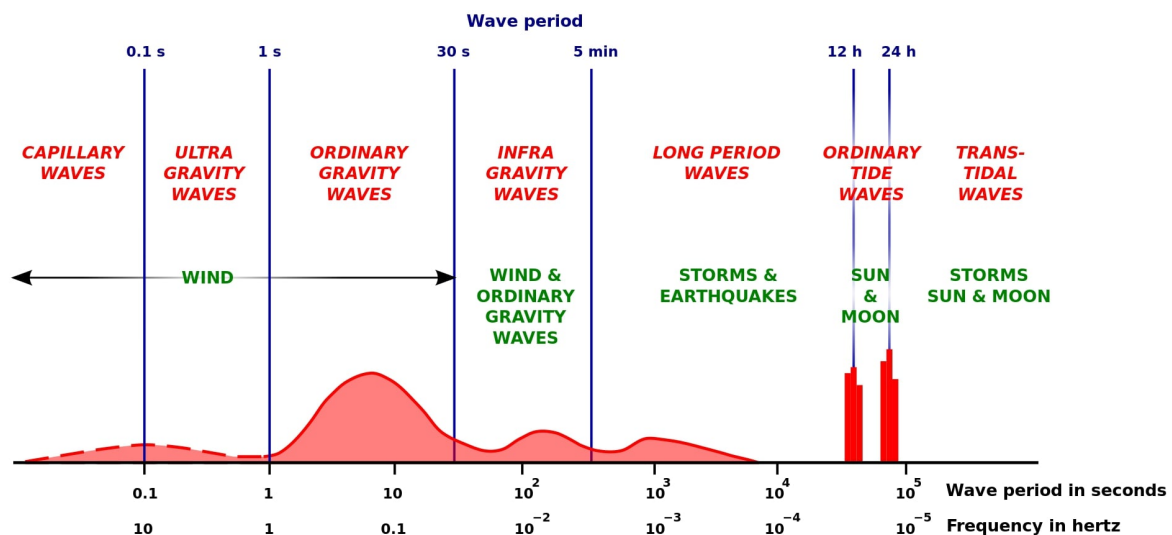


Figure 2.1: Classification of the spectrum of ocean waves according to wave period

The spectrum above shows that the most frequent type of waves are created by the wind and have periods between 5 and 20s approximately which corresponds to wavelengths going between 40 and 620m.

In linear theory, waves carry energy horizontally but no matter. When waves become too steep or the

water is too shallow, waves break and transport matter. In that case, the problem is not linear at all anymore. In the literature, waves are represented as long crested regular waves. However, this is a simplification compared to reality as most ocean waves are irregular and short crested. The picture below shows the difference:

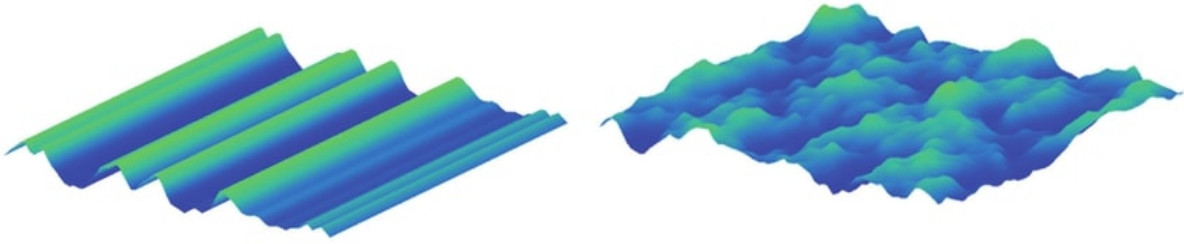


Figure 2.2: Comparison between long and short crested waves

When studying the wave added resistance, a deep water scenario is assumed. This is true when $\lambda/2 < d$ where d is the depth. This case is true in most places in the sea with ordinary gravity waves. From that assumption and some wave parameters, it is possible to derive a few interesting equations relating the wave speed, period and length. Another important parameter is the significant wave height H_s . In statistics, it is defined as the average of the largest 33% of waves. It is also roughly equal to a visual estimate of the waves' height. The following formulae link the aforementioned variables:

$$\begin{aligned}\lambda &= \frac{gt^2}{2\pi} \\ V_c &= \frac{\lambda}{t}\end{aligned}\tag{2.1}$$

Eventually, when waves hit a ship, the wave incident angle α is a crucial parameter. It seems that the way it is defined is not always the same depending on the article. Therefore, in this report α will be defined as equal to 0° when the ship sails through head waves i.e the waves come from the bow and go in the opposite direction of the ship, and α will be equal to 180° when it is sailing through following waves. Eventually, this problem can be considered as symmetrical. In case of oblique waves, it does not make any difference in terms of absolute value of the wave added resistance if they come from portside or starboard. Therefore, the incident wave angle can only reach values between 0° and 180° . In every case, the wave added resistance is defined as positive when it goes against the forward movement of the ship and negative when it goes with the ship.

The added resistance is usually plotted as a function of the ratio between the wave length λ and the length between perpendiculars L_{pp} , $\frac{\lambda}{L_{pp}}$. It can also be plotted as a function of the Froude number F_r . The associated non dimensional coefficient C_{AW} is defined as such:

$$C_{AW} = \frac{R_{AW}L_{pp}}{\rho g \zeta^2 B^2}$$

As an example, the graph below shows different values of the added resistance coefficient depending on the wavelength to L_{pp} ratio for different ship models [32]:

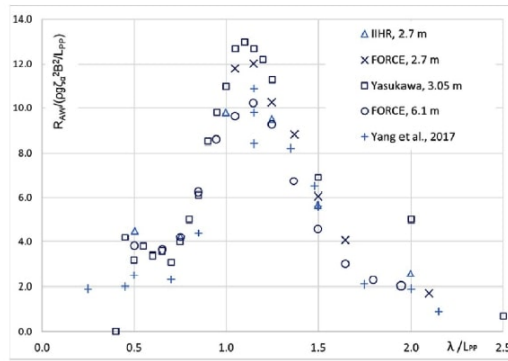
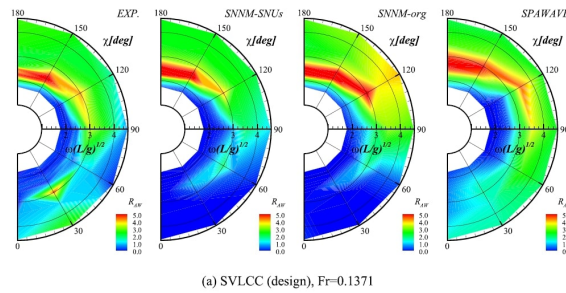


Fig. 1. Measured dimensionless added resistance coefficient of KCS ship in head waves at different tanks, $Fr = 0.26$.

As it can be seen from the figure, there is usually a resonance point when λ is close to L_{pp} . Most studies focus on head waves as it is the worst case scenario. However, some models have been developed for all wave angles. Polar diagrams enable to show the influence of the wave angle in the added resistance as shown below [23]:



(a) SVLCC (design), $Fr=0.1371$

It also highlights the fact that for following waves at low speed, the added resistance can actually be negative, and in that case the wave "pushes" the ship. Eventually, it is also common to find 3D plots of the added resistance or its non dimensional equivalent coefficient as a function of $\frac{\lambda}{L_{pp}}$ and the incident angle [32]:

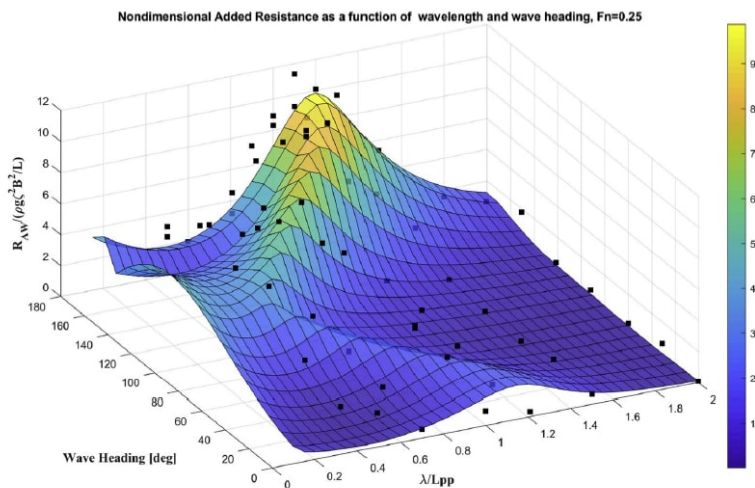


Fig. 18. Experimental (black square marker) and predicted (colour surface) added resistance of the S175 ship in design condition in regular waves of various headings, $Fr = 0.25$. (For interpretation of the references to colour in this figure legend, the reader is referred to the Web version of this article.)

In the graph above, it is possible to see the non dimensional wave added resistance with a peak of

resonance where the wavelength is approximately equal to the length between perpendiculars and for a head wave. As mentioned earlier, this is the worst case scenario.

Scientists started assessing the value of wave added resistance in the 40's [19]. Since then, different methods have been developed to quantify the wave added resistance and give analytical formulas with different hydrodynamics approach during the second half of the 20th century [35] [34] [36] [33] [26] [17] [48]. Most of these methods are still used as benchmarks to develop more accurate numerical solutions. Overall, these methods can give a pretty good approximation for the added wave resistance and have been widely used and improved by scientists. However, this problem is very complex in terms of number of influential parameters (from the waves, the ship, the hull etc) and as it includes non linear phenomena. It is also important to note down that they focus on regular waves, i.e the wave signal is sinusoidal and the wave parameters (wave length, period and amplitude) remain constant. Therefore, some experiments have been done in towing tanks and in full scale conditions to try to validate and/or adjust the theoretical formulas. Furthermore, studies have attempted numerical resolutions of the problem with CFD.

2.1.2. Numerical and experimental resolution

With the rapid progress of computer power, there is an increasing use of CFD to solve the issue of wave added resistance.

One method consists in using an Unsteady Reynolds Averaged Navier-Stokes (URANS) and Detached Eddy Simulation (DES) method with six degrees of freedom for various Froude numbers and wave lengths but only in head waves conditions [49] [46]. The results are compared with experimental data from a KVLCC2 bare hull and a post-Panamax 14000 TEU containership known as Duisburg Test Case (DTC) [49]. The added resistance is validated for a large range of wave lengths.

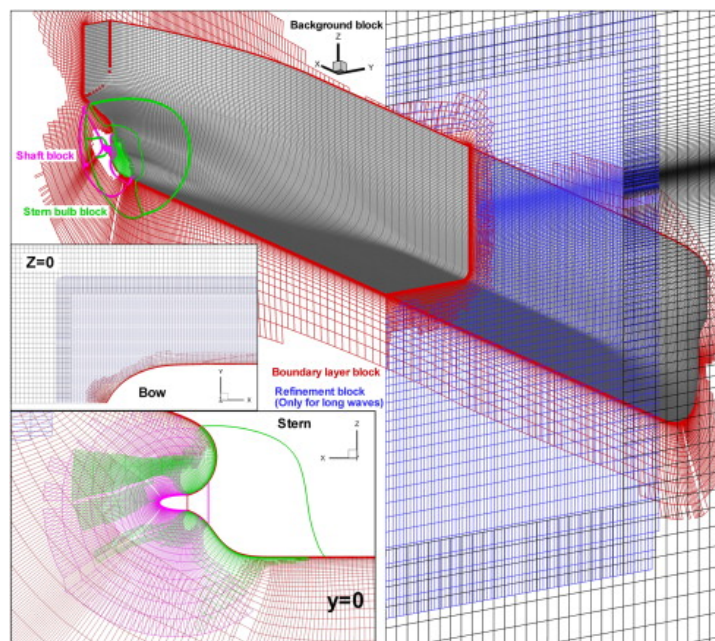


Figure 2.3: Overset grid system developed by Sadat-Hosseini [46]

In the CFD resolution shown above, the number of grid points goes up to 13.1M in long waves ($0.6 < \lambda/L_{pp} < 2.0$) and 45.1M for the shortest waves ($\lambda/L_{pp} = 0.1810$). It enables to have results for different wave length and to compare them with experimental data and analytical resolution:

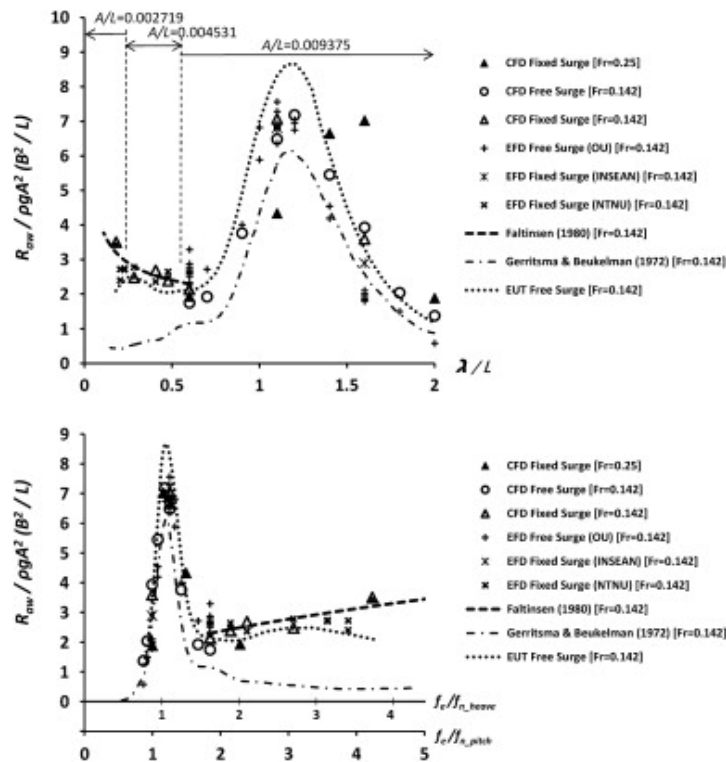


Figure 2.4: Added resistance at $F_r = 0.25$ and $F_r = 0.142$ [46]

But CFD also gives the resistance distribution along the hull which can also be very interesting for hull design:

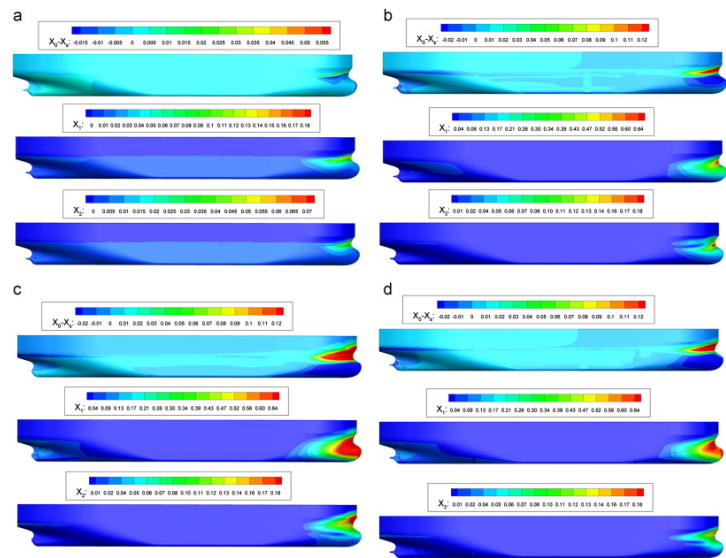


Figure 2.5: Amplitude of resistance along the hull for different wavelengths [46]

Here, we can clearly see the added resistance on the bulbous bow from head waves.

Other research involve a momentum conservation method based on strip theory and/or a 3D Rankine panel method (direct pressure integration) to derive the added wave resistance [43] [25]. Here, both methods are used and compared with experimental results. A potential flow method like the strip based method requires an analytical formula. The scientists used the one derived from Maruo's momentum

conservation equation. As it is not very accurate for short waves, Faltinsen's method [14] is used in this range. For the 3D Rankine panel based method, the second order pressure is directly integrated over the mean body surface. The results are then again compared to experimental tests:

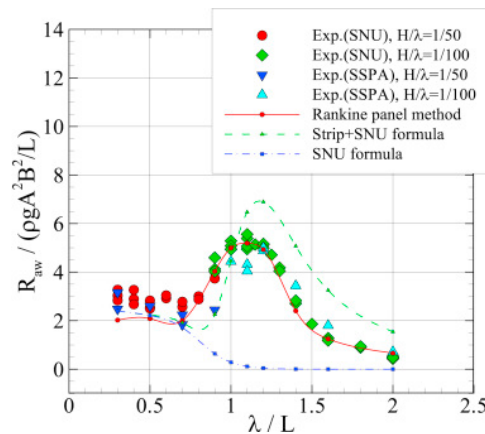


Figure 2.6: Wave added resistance, $F_r = 0.137$, S-VLCC[43]

These methods are also widely used because there are considered to have a shorter computational time than CFD while still having accurate results. Moreover, the simulations and experiments were done for different wave angles. Again, it shows good agreement with the experimental results.

The numerical methods are improving in terms of accuracy. However, there are still uncertainties especially in short waves as it becomes difficult to differentiate the calm water resistance from the wave added resistance and non-linear phenomena such as viscosity must be taken into account [57] [12]. In order to have a correct accuracy, fine grid are needed which is also very time consuming, thus making CFD difficult to implement for a direct industrial application. CFD simulations for long journeys cannot be computed. So far, it has mostly been used in regular head waves which is less realistic than irregular waves in arbitrary directions.

Whether scientists try to solve the added resistance analytically or numerically, experimental data are always required to validate the results. Experiments require model ships and towing tanks which can produce waves and are usually costly and time-consuming. Another method could be to use actual data from in-service ships although information from companies are rarely open access [40] [39].

Over the years, the total database of added resistance is composed of around 130 ships [32]. Among the sample points, around 50% of them were made in head waves. Some of these tests have open access data and are widely used as benchmarks for theoretical or numerical validation.

The Wigley type ship is one of the most tested ship hull but mostly in head waves [27] [16] [28]. The series 60 ship has also been tested in various wave headings [53]. As well, many experiments were conducted with a S175 model ship for various wave headings and different Froude numbers [15] [51]. Eventually, the KVLCC2 ship is also a pretty common model ship [9] [32]. As a note, the empirical formula developed by Jinkine and Ferdinande shows another way of using experiments [24]. The typical dimension for these models ranges between 1 and 3m [20]:

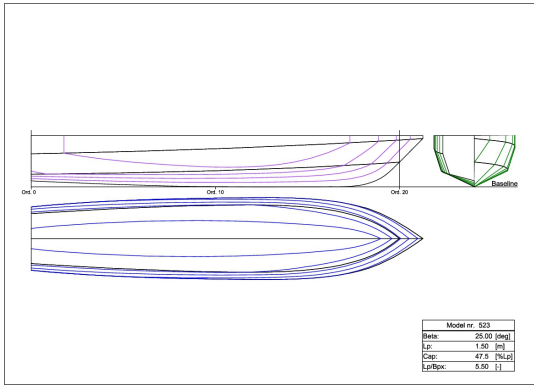


Figure 2.7: Line plan of the model

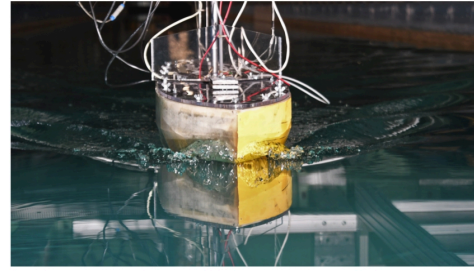


Figure 2.8: Model ship in towing tank

Towing tank experiments enable to observe the complete physics behind the wave added resistance phenomenon and are a good tool to validate results. However, large uncertainties remain within these experiments. The accuracy and number of samples depend on many parameters such as the quality of the sensors, the length of the towing tank, its ability to make waves etc. On a model, the measured forces are relatively low therefore the sensors need to be very accurate. This is, in fact, a very important challenge especially for relatively short waves ($\lambda/L \approx 0.5$) as it is the most common type of waves ships now encounter. Moreover, the scale issues that appear are usually not considered although it is of important matter especially when viscosity plays an important role. In towing tanks capable of producing waves with multiple directions, the size of the tank can also be an issue. The ship speed can also be limited depending on the basin. Eventually, different methods and materials make the experiments difficult to compare. [32].

Another method is to retrieve actual data from in-service ships. The mean added resistance is defined as the difference between the propulsive force of the ship and the sum of the calm water resistance and the wind resistance:

$$\bar{R}_{AW,emp} = \frac{P_b}{STW} \times \eta_D \eta_M - R_{T,calm} - R_{wind} \quad (2.2)$$

The required data can be collected by sensors on the ship such as anemometers and Doppler velocity (for wind speed and direction and speed through water respectively) while ship dimensions are measured or provided by the shipping company. It is interesting to retrieve such values from full scale ship in real life sea conditions, however there are still large uncertainties from the data. The calculation for the added resistance is based on linear theory although a ship sailing in open sea has a non-linear behaviour. Therefore, all non linear phenomena such as slamming or propeller load fluctuations were neglected. Some parameters such as the propulsive and transmission efficiencies can be hard to acquire. The sensors used are also put through harsh conditions and can get destroyed or freeze if the ship goes through a storm or in very cold areas. Depending on the temperature, the properties of seawater can also be affected [39]. These data are all collected to validate numerical or analytical calculations and some are considered as benchmarks. One can note that it might bias results towards head waves and for wave lengths approximately the sizes of the ships [38].

2.1.3. Semi empirical methods

As a third option, it is possible to find semi-empirical formulae by simplifying the analytical equations and by modifying these equations with adjustment coefficients from empirical data. One of the main benefit of the semi-empirical method is that it can be easily implemented for an industrial use and it requires very little computational time. On the other hand, the accuracy is limited as the shape of the

hull is usually kept very simple. The equation only involves simple ship dimensions such as draught or length between perpendiculars and wave parameters such as the wave heading and the wave period.

Multiple joint projects have tried to estimate the wave added resistance for a direct use by the industry. Among others, we can cite the SHOPERA-EU project or the NMRI method which is also widely used and recommended by the IMO (international maritime organisation).[54]. It is also a concern for the ITTC (international towing tank conference).

In the context of routing computation and performance prediction, the team has to evaluate the wave added resistance for a very large amount of case scenarios (some files can exceed a million lines, each line being a case with different wind/wave parameters and ship speed or sail configurations). Therefore, the computation must be fast. Furthermore, as it is used during the conception phase, the full design of the ship might not be completed. That is why it is also important to have relatively simple ship parameters (such as length and beam) rather than an accurate hull design that could be subject to change. With these factors in mind, semi-empirical methods to assess the wave added resistance were considered the most adequate solutions to fulfill this mission.

2.1.4. State of the art and scope for this thesis

So far, most models focus on head wave resistance for monohulls [8]. Another aspect of study is the wavelength, especially the λ/L_{pp} ratio. Research usually focuses on one specific range of wavelengths and the most commonly studied one is for:

$$\lambda/L_{pp} \approx 1 \quad (2.3)$$

This is also the range and wave angle for which the experimental data is the most important. In fact experiments with other wave angle requires specific towing tanks which are more complex and costly to set up. Therefore, the empirical data used to adjust to formulas may have a bias towards head waves with a wavelength close to the ship's length.

In the context of wind-assisted ships, it is important to highlight a few limits. The models were developed for non sail-equipped monohull ships. Therefore, the potential impact of the sails on the ship's balance such as leeway or heel are not taken into account. The added resistance due to the interaction between the sails, the hull and the rudder is also neglected. Few research has been done about the influence of heel or leeway but the results were mostly compared with numerical solutions [44] [47]. As for an example, Canopée has a heel of about a few degrees (2 to 3°). This could be a field of research for the future but it will also be neglected in this case.

The criteria of selection for the semi-empirical models will be depicted below. Once there are chosen, the goal will be to compare them and be able to choose the "best" one for each case. This has been briefly done before [62] but it is now important to check if these comparisons are verified for VPLP's ships.

2.2. Importance of quantification for performance prediction

2.2.1. Influence on fuel consumption

The added resistance due to weather conditions is usually estimated to reach about 15-20% of the calm water resistance. Although this is already large enough to be a great concern for conventional ships, it may be even more important for sailing ships. This is due to the fact that the waves involved in the process are generated by the wind.



Figure 2.9: Fuel consumption without waves and extra fuel consumption from waves

The figure above highlights this phenomenon. The x-axis represents the distance traveled by a certain wind-assisted ship and the y-axis represents the instantaneous power required to propel the ship at a fixed speed. The plot in blue represents the power required when the wave added resistance is not taken into account but the ship uses the wind to reduce its fuel consumption. The red plot represents the added power necessary to counteract the wave added resistance. Therefore, the total required power can be found by adding the two plots. After around 900nm, the calm water power and the wave added power are almost equal ($\approx 600kW$). On the other hand, the former is almost constant for the end of the trip ($\approx 1400kW$) while the latter is almost equal to 0. Although, the 15-20% figure is relatively accurate as an average, the figure shows that the wave added resistance can vary very much from that number, ranging from 0 to 100 % of the calm water resistance.

At around 1600nm, the required calm water power is negative, suggesting that the wind conditions are good enough for the ship to be exclusively propelled by its sails. However, the wave added power is especially large in this case. As mentioned before, in this case, good wind conditions imply bad wave conditions. Overall, when the engine must deliver more power (i.e the sails are not delivering any thrust), the wave added resistance is relatively low which could be contradictory for a conventional ship.

In this example, one can see that aiming for the best wind conditions without taking into account the wave added resistance might not be the most efficient method or could even be counterproductive. This is why it is so important to assess it correctly so that the routing software can optimize efficiently the trip.

2.2.2. Criteria of selection

The semi-empirical models must verify a few conditions in order to be selected:

- All the equations must be explicitly developed and all the variables must be depicted. (Otherwise, it is almost impossible to program them)
- The models must only require relatively simple ship parameters such as length, beam or draught. Complex hull designs would require a more detailed numerical solution which would have a great impact on computational time.
- The models must be usable for all ranges of wavelengths that ships might encounter.
- They must be able to evaluate the wave added resistance for all wave angles. Most of the research (analytical, numerical and experimental) has been on head waves. However, the incident wave angle may have a large influence on the final result. While head waves are usually the worst case scenario, in certain conditions following waves can even give a negative resistance i.e "push" the ship. Therefore, it is important to model all case scenarios. Furthermore, depending on the trip and the region, wave angles can be either very irregular such as in the Mediterranean sea or pretty uniform such as in the

Atlantic Ocean. Models must be relevant in both cases. These differences will be highlighted in the 4th chapter on the optimized tool for metoceanic analysis.

-Some authors have developed some methods but continued to improve them. If possible, the models should be the newer version.

With these requirements, four models were chosen. Two of them are original models. The third one reuses one of them and adjusts it for certain study cases. Some empirical factors have different values but the method and equations are the same. The fourth one is a meta-model which tries to take the best of both aforementioned models. They are all depicted below.

2.3. Appropriate models for the project

2.3.1. First and second model: Liu and Papanikolaou (2021) and Mittendorf et al. (2023)

One of the most recent semi-empirical formula comes from Liu and Papanikolaou with multiple articles between 2011 and 2020 [31], [30], [52], [32]. It has been validated by other studies and is now recommended by the ITTC Ship Operation at sea specialist committee for the wave correction during sea trials [55], [39]. Their method is inspired from Jinkine and Ferdinand's empirical formula [24] that is well adapted for long waves. It uses Faltinsen's asymptotic formula for short wave lengths [14]. The pressure terms are directly integrated along the ship's hull which yields:

$$R_{AW} = \int_C \bar{F}_e \sin(\theta) dl \quad (2.4)$$

And

$$\bar{F}_e = \frac{1}{2} \rho g \zeta_A^2 (\sin(\theta + \alpha))^2 + \frac{2\omega V}{g} [1 - \cos(\theta) \cos(\theta + \alpha)] \quad (2.5)$$

This second order drift force is integrated along the non-shadowed area of the waterline. This area is the part of the hull that is directly in contact with the incident waves as described in the figure below. This formula is then simplified to obtain a formula that doesn't require all the information of the hull and which is explained further.

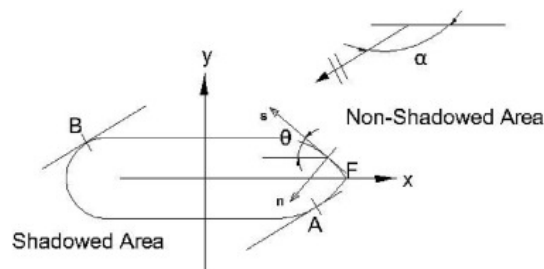


Figure 2.10: Coordinate system and example of shadow area

It is important to elaborate on a specific case study: following waves with a relatively small ship speed. When the ship speed is smaller than half of the wave's group velocity, then the added resistance is negative i.e the waves are "pushing" the ship. When it is equal to half of the wave's group velocity ($V_g/2$ or $V_c/4$), the added resistance will be equal to 0. Eventually, when the ship's speed is equal to or larger than $V_c/2$, the ship "catches up" with the wave in front of him and therefore, the added resistance becomes positive. In that case, it is considered to be added resistance from head waves at a speed: $U - V_c/2$.

In various headings, the added resistance is divided between the ship motion component R_{AWM} and the diffraction component R_{AWR} . These two values are depicted below.

Ship motion component:

$$R_{AWM} = 4\rho g\zeta^2 \frac{B^2}{L_{pp}} a_1 a_2 a_3 \bar{\omega}^{b_1} \times \exp\left(\frac{b_1}{d_1} (1 - \bar{\omega}^{d_1})\right) \quad (2.6)$$

These empirical adjustments were first developed by Jinkine and Ferdinande (1974) [24] and have been continuously improved.

a_1 is an amplitude factor which has been modified since its introduction in 1974. It is now equal to:

$$a_1 = 60.3 C_B^{1.34} (4k_{yy})^2 \left(\frac{0.87}{C_B}\right)^{-(1+F_r)\cos(\alpha)} \left(\ln\left(\frac{B}{T_{max}}\right)\right)^{-1} \frac{1 - 2\cos(\alpha)}{3} \quad (2.7)$$

In beam to head waves. In following waves, it will be a function of the ship speed and the wave's group velocity as described earlier. Eventually, the authors assume a linear interpolation between the following and beam waves.

a_2 is a speed correction factor and is solely dependent on the Froude number. It is valid for $0 \leq F_r \leq 0.3$ but considering the sizes and the speed of the studied ships (between 100 and 400m for conventional speeds of 10 to 20 kn), this factor should not be out of its validation range.

$$a_2 = \begin{cases} 0.0072 + 0.1676F_r & \text{if } F_r < 0.12 \\ F_r^{1.5} e^{-3.5F_r} & \text{if } F_r \geq 0.12 \end{cases} \quad (2.8)$$

The authors have highlighted the influence of trim in the added resistance [52] due to the inclined bottom surface. A trim factor is therefore introduced to take this effect into account in the formula and is called a_3 :

$$a_3 = 1.0 + 0.25 \arctan\left(\frac{|T_a - T_f|}{L_{pp}}\right) \quad (2.9)$$

The frequency factor $\bar{\omega}$ is more complex and depends on many different parameters. Its formula has also been developed along the years. Here is the latest version from Liu and Papanikolaou 2020 [32]:

$$\bar{\omega} = 2.142 \sqrt[3]{k_{yy}} \sqrt{\frac{L_{pp}}{\lambda}} \left[1 - \frac{0.111}{C_B} \ln\left(\frac{B}{2.75T_{max}}\right)\right] \left(\frac{C_B}{0.65}\right)^{0.17} [(-1.377F_r^2 + 1.157F_r)|\cos(\alpha)| + \frac{0.618(13 + \cos(2\alpha))}{14}] \quad (2.10)$$

Eventually, b_1 and d_1 are empirical coefficients which depend on $\bar{\omega}$ and the parameters of the ship:

$$b_1 = \begin{cases} 11.0 & \text{if } \bar{\omega} < 1 \\ -8.5 & \text{if } \bar{\omega} \geq 1 \end{cases} \quad (2.11)$$

$$d_1 = \begin{cases} 566 \left(\frac{L_{pp} C_B}{B}\right)^{-2.66} & \text{if } \bar{\omega} < 1 \\ -566 \left(\frac{L_{pp} C_B}{B}\right)^{-2.66} \times \left(4 - \frac{125 \operatorname{atan}|T_a - T_f|}{L_{pp}}\right) & \text{if } \bar{\omega} \geq 1 \end{cases} \quad (2.12)$$

Overall, the ship motion component of the wave added resistance takes into account, the ship speed, the trim, the amplitude and the resonance frequency. This formula is a general case that can be applied to any wave heading. Likewise, the authors have proposed an improved formula for the diffraction component of added resistance.

Diffraction effect component:

The diffraction effect component is divided in four different segments which are then added up to form the total added resistance from reflection. Each segment is depicted in the figure below. Depending on the wave heading, some segments will be in the shadowed area and thus will not be taken into account.



Figure 2.11: Segment and parameters definition

The formulas for each segment are:

$$R_{AWR}^1 = \frac{2.25}{4} \rho g B \zeta^2 \alpha_T [\sin^2(E_1 - \alpha) + \frac{2\omega U}{g} (\cos(E_1)\cos(E_1 - \alpha) - \cos(\alpha))] \left(\frac{0.87}{C_B}\right)^{(1+4\sqrt{F_r})f(\alpha)}$$

if $E_1 < \alpha < \pi$

$$R_{AWR}^2 = \frac{2.25}{4} \rho g B \zeta^2 \alpha_T [\sin^2(E_1 + \alpha) + \frac{2\omega U}{g} (\cos(E_1)\cos(E_1 + \alpha) - \cos(\alpha))] \left(\frac{0.87}{C_B}\right)^{(1+4\sqrt{F_r})f(\alpha)}$$

if $\pi - E_1 < \alpha < \pi$

$$R_{AWR}^3 = -\frac{2.25}{4} \rho g B \zeta^2 \alpha_T [\sin^2(E_2 + \alpha) + \frac{2\omega U}{g} (\cos(E_2)\cos(E_2 + \alpha) - \cos(\alpha))]$$

if $0 < \alpha < \pi - E_2$

$$R_{AWR}^4 = -\frac{2.25}{4} \rho g B \zeta^2 \alpha_T [\sin^2(E_2 - \alpha) + \frac{2\omega U}{g} (\cos(E_2)\cos(E_2 - \alpha) - \cos(\alpha))]$$

if $0 < \alpha < E_2$

(2.13)

Besides the known parameters, α_T adds the influence of the ship's draft. E_1 and E_2 are the average entrance angle and run angle respectively ($E_1 = \arctan(\frac{B}{2L_e})$ and $E_2 = \arctan(\frac{B}{2L_r})$). For a better understanding of what the length of entrance L_e and the length of run L_r mean, the figure below shows how they can be measured [62]:

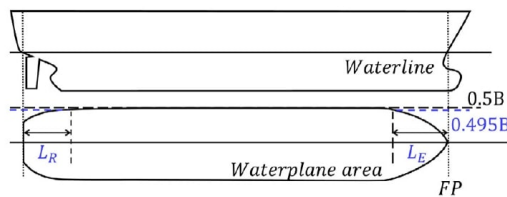


Figure 2.12: Definition of length of entrance and run

α is not in the considered range of angle, than the value of the component is neglected. Eventually, the total resistance created by diffraction is:

$$R_{AWR} = \sum_{i=1}^4 R_{AWR}^i \quad (2.14)$$

which yields:

$$R_{Total} = R_{AWM} + R_{AWR} \quad (2.15)$$

This study was made during the SHOPERA-EU project which aimed to find rational calculation of the hydrodynamic behavior of ships in waves.

Since its publication, it has been widely used. A notable enhancement of this calculation was published by Mitendorf et al. in 2023 [38]. It follows the same idea but some empirical parameters are adjusted. Moreover, it focuses on the uncertainties within the experiments and the calculations and provides values with upper and lower estimation boundaries. These empirical parameters depend on the block coefficient. In fact, a new set of ships and data points were used and the dataset was divided between slender and blunt ships ($C_b < 0.7$ and $C_b > 0.7$ respectively).

2.3.2. Third model: Lang and Mao (2021)

The Lang and Mao article from 2021 [60] proposes to solve the wave added resistance in arbitrary waves with a different method. Likewise, this method is semi-empirical, it uses a theoretical formula and adjusts it with additional parameters to fit the experimental data. They developed a formula called CTH (Chalmers Tekniska Högskola) which is based on the NMRI formulae for waved added resistance created by diffraction [15] and on Jinkine and Ferdinande [24] for the ship motion induced wave resistance.

Ship motion component:

The latter's expression is given in the equation below:

$$R_{AWM} = 4\rho g \zeta^2 \frac{B^2}{L_{pp}} \bar{\omega}^{b_1} \exp\left[\frac{b_1}{d_1}(1 - \bar{\omega}^{d_1})\right] a_1 a_2 \quad (2.16)$$

The adjustment factors act exactly as in Liu and Papanikolaou's article, however, there are calculated differently. The frequency factor now has two expressions depending on the Froude number:

$$\bar{\omega} = \begin{cases} \frac{\sqrt{L_{pp}/g} c_1 \sqrt{k_{yy}} 0.05^{0.143}}{1.09 + \lceil \frac{k_{yy}}{0.25} \rceil 0.08} & \text{if } F_r < 0.05 \\ \frac{\sqrt{L_{pp}/g} c_1 \sqrt{k_{yy}} F_r^{0.143}}{1.09 + \lceil \frac{k_{yy}}{0.25} \rceil 0.08} & \text{if } F_r \geq 0.05 \end{cases} \quad c_1 = 0.4567 \frac{C_B}{k_{yy}} + 1.689 \quad (2.17)$$

a_1 is the amplitude factor and is equal to $60.3 C_B^{1.34} (\frac{1}{C_B})^{1+F_r}$. a_2 is also a speed correction factor in this case. Its expression is highly dependent on the Froude number:

$$\bar{\omega} = \begin{cases} 0.0072 + 0.24 F_r & \text{if } F_r < 0.12 \\ F_r^{-1.05} C_B^{2.3} \exp\left[(-2 - \lceil \frac{k_{yy}}{0.25} \rceil - \lfloor \frac{k_{yy}}{0.25} \rfloor) F_r\right] & \text{if } F_r \geq 0.12 \end{cases} \quad (2.18)$$

Eventually, b_1 and d_1 are adjustment factors that are depicted in the original article [60]. One can observe that the result shown above does not depend on the incident wave angle. This case is only for head waves and is described in a previous articles from Lang and Mao [61]. Thus, the main focus of this article [60] is to adapt this formula at arbitrary heading angles. Therefore, the ship motion induced wave resistance in head waves is modified to fit for any wave heading as such:

$$R_{AWM}(\alpha) = R_{AWM}(180) \times \exp\left(-\left(\frac{\alpha}{\pi}\right)^{4\sqrt{F_r}}\right) + \rho g \zeta^2 \frac{B^2}{L_{pp}} \left[\frac{\lambda}{B} \max(\cos(\alpha), 0.45)\right]^{-6F_r} \sin(\alpha) \quad (2.19)$$

Diffraction effect component:

In head waves, R_{AWR} is described as such:

$$R_{AWR} = \frac{1}{2} \rho g \zeta^2 B B_f \alpha_T (1 + \alpha_U) \frac{0.19}{C_B} \left(\frac{\lambda}{L_{pp}} \right)^{F_r - 1.11} \quad (2.20)$$

Apart from the aforementioned parameters, B_f is a bluntness coefficient equal to $2.25 \sin^2(E)$ with $E = \arctan\left(\frac{B}{2L_e}\right)$. α_T is also the draft coefficient but its expression is different than in Liu and Papanikolaou's research: $\alpha_T = 1 - e^{-2k_e T}$ and $k_e = k \left(1 + \frac{\omega V}{g} \cos(\beta)\right)^2$. Eventually, $1 + \alpha_U$ is an advance coefficient with $\alpha_U = C_U F_r$ and $C_U = \max(-310 B_f + 68, 10)$. Likewise, this formula is only valid for head waves. In this paper, a new formula enables to calculate the added resistance from wave diffraction for an arbitrary wave angle:

$$R_{AWM}(\alpha) = \begin{cases} R_{AWM}(180) \times F_r^{([\cos(\alpha)] - [\cos(\alpha)]) F_r} \cos(\alpha) & \text{if } 0 \leq \alpha < 90 \\ R_{AWM}(180) \times F_r^{-1.5([\cos(\alpha)] + [\cos(\alpha)]) F_r} \cos(\alpha) & \text{if } 90 < \alpha \leq 180 \end{cases} \quad (2.21)$$

The authors also mentioned how the peak resonance frequency shifts with the incident wave angle. In fact, when α decreases (from head waves to beam then following waves), the wavelength value for which R_{AW} is maximum tends to decrease. To account for this phenomena, a new frequency correction factor is introduced:

$$\omega_\alpha = \bar{\omega} \times C_\omega(\alpha) \quad (2.22)$$

where the numerical values of $C_\omega(\alpha)$ can be found in the article for each α . This new formula has been validated by full-scale measurement data from three different ships, a chemical tanker, a PCTC (pure car, truck carrier) and a container ship. This method is also convenient as it is very easy to implement and requires very little information from the ship.

Eventually, they introduced a last parameter from different observations to compensate the increase in resistance in large waves in the case of irregular waves. A ship's response in real sea conditions is nonlinear which can reduce its efficiency. In large waves, it can also be subject to surfing. That is why the authors use a wave height based correction factor in the case of irregular waves [60] (the calculation of irregular wave resistance will be depicted in the next section):

$$C_{H_s} = \sqrt[3.5]{H_s} \quad (2.23)$$

Therefore, the total added resistance will be:

$$R_{tot,irr} = R_{irr} C_{H_s} \quad (2.24)$$

2.3.3. Fourth model: Kim and Kim (2022)

The last notable semi-empirical method was published in 2022 by Kim et al [62]. It consists in a meta-model created by fusing the two methods presented before. The article first compares both methods and another, the "STA2" method from Boom et al [21] used by the IMO. The last one is not as useful for a direct use as it is only valid for head waves. The wave added resistance from Liu and Papanikolaou and from Lang and Mao will be denoted as $R_{AW,LP}$ and $R_{AW,CTH}$ respectively. The inputs for this method are the ones from the previous models but it also has different parameters depending on the ship type. In fact, different datasets were used for each ship type so the numerical values of the empirical

parameters differ from one type to another. These ship types are supposed to represent a broad range of the world fleet (tanker, liquefied gas, bulk carrier, general cargo, container ship, Ro-Ro and ferry).

For head, beam and following waves, the wave added resistance is calculated as such:

$$R^i = [1 - g(\lambda/L_{pp})]R_{AW,CTH}^i + g(\lambda/L_{pp})R_{AW,LP}^i \quad (2.25)$$

where i is either head ($\alpha = 180$), beam ($\alpha = 90$) or following ($\alpha = 0$) waves and g is a hyperbolic function:

$$g(\lambda/L_{pp}) = \frac{1}{2}(1 + \tanh(a(b - \frac{\lambda}{L_{pp}}))) \quad (2.26)$$

Here, a and b are parameters dependant on the ship type and can be found in the original article.

Once the calculation is done for all three different angles, the final wave added resistance for an arbitrary wave angle α is:

$$R_{AW}(\alpha) = \begin{cases} (1 - f(\alpha))R^{head} + f(\alpha)R^{beam} & \text{if } 90 \leq \alpha < 180 \\ (1 - f(\alpha))R^{beam} + f(\alpha)R^{following} & \text{if } 0 < \alpha \leq 90 \end{cases} \quad (2.27)$$

Here, f is equal to:

$$f(\alpha) = \frac{1}{2}(1 + \tanh(c(d - \alpha))) \quad (2.28)$$

Once again, c and d depend on α and the ship type and can be found in the original article. The new model is supposed to follow the CTH model's behaviour in short waves and the LP model's behaviour in long waves.

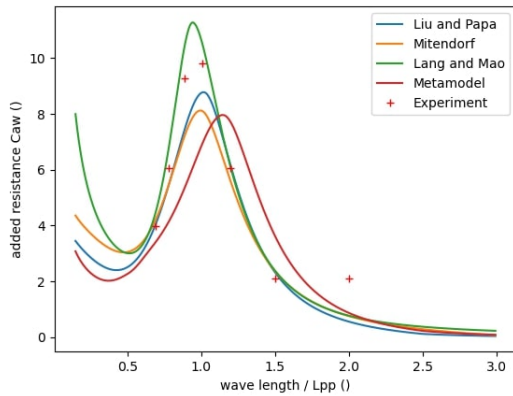
In general, these four methods provide a good estimate of the wave added resistance in arbitrary wave headings. However, all highlight the fact that the amount of full scale measurement data is quite small and more studies would help to enhance the accuracy of these semi-empirical formula. It could also be interesting to use the formula from Mitendorf [38] in the meta-model created by Kim [62] instead of the one from Liu and Papanikolaou [32].

2.3.4. Program verification and methodology

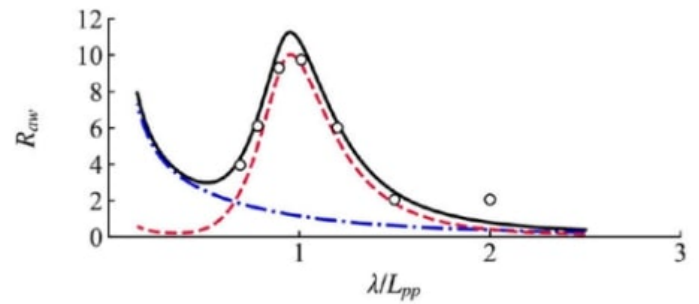
The articles provide all the equations to implement the wave added resistance. However, it is more complex to verify these results. The experimental data used to adjust and/or validate the models are usually complicated to retrieve. Therefore, the main verification process was through the provided graphs. For that, the last two articles had the most interesting graphs to compare our results. The next graph shows the comparison between our models and the one from Lang and Mao for the case of a S175 ship, a common model container ship used in towing tanks which main parameters are displayed below:

L_{pp} (m)	175
B (m)	25.4
T (m)	9.5
C_b []	0.572
l_e (m)	59.05
k_{yy} []	0.24

Table 2.1: S175 ship parameters



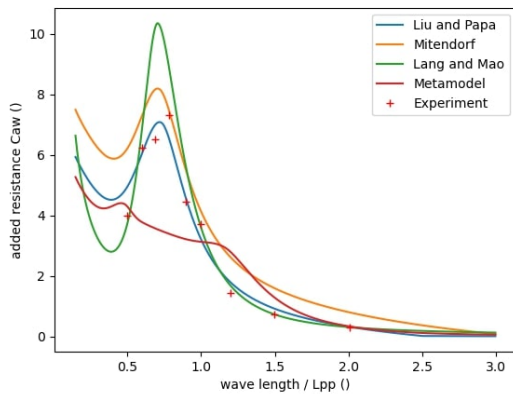
(a) Results from the program of all models



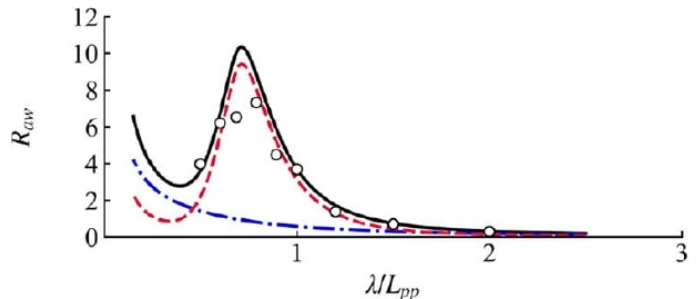
(b) Results from Lang and Mao [60]

Figure 2.13: Non dimensional wave added resistance, ship: S175, $\alpha = 150^\circ$, $F_n = 0.25$

On the right graph, the red figure represents the ship motion component of the wave added resistance while the blue figure represents the wave reflection effect component. The black one is the sum of both and the total wave resistance. Although the dimensions may alter the form of the graph, it matches the green figure from the left graph which is our implementation of this model. We can also see how the other models behave. As predicted, Mittendorf and Liu and Papanikolaou are very similar. The same experiment was conducted with a wave incident angle of 120° .



(a) Results from the program of all models



(b) Results from Lang and Mao [60]

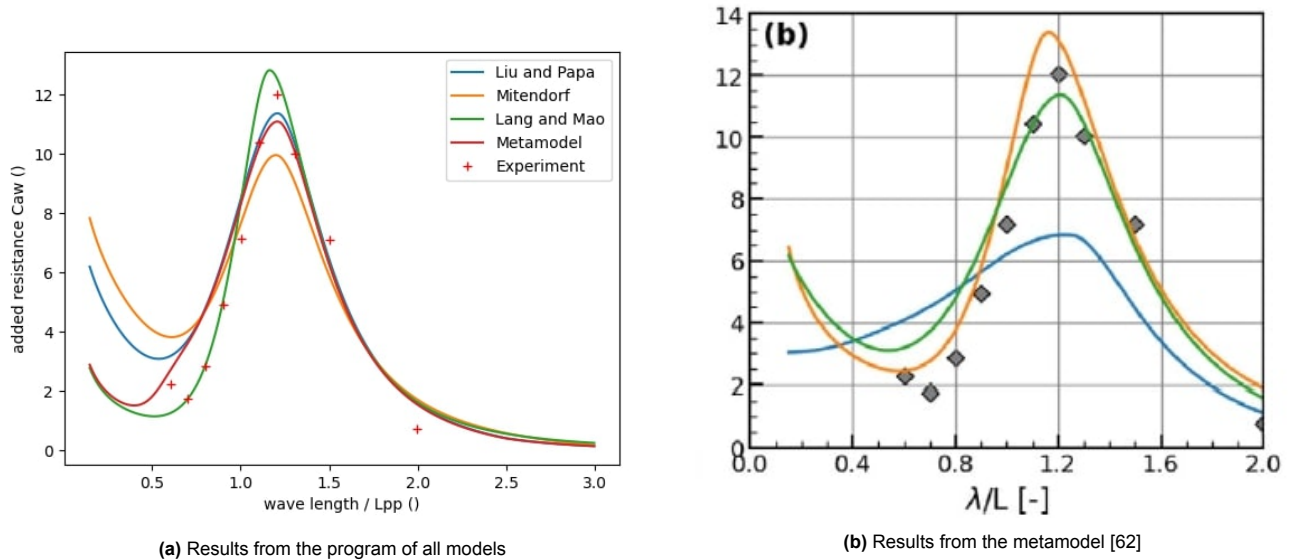
Figure 2.14: Non dimensional wave added resistance, ship: S175, $\alpha = 120^\circ$, $F_n = 0.25$

One can observe that the green figure from the left graph matches the black one from the right graph. Furthermore, they both tend to overestimate the wave added resistance at the peak in this case. The left graph also enables to show one of the limits of the meta model. In some cases, the meta model does not implement the peak resistance. As the wave angle shifts towards the beam of the ship, we can also observe how the peak also shifts towards a lower wavelength.

In order to verify the other models, graphs from the meta model article were used. Among those, one was made with data points from the S175 model while the other one used data points from another model ship, the S60 which is presented as a general cargo ship:

L_{pp} (m)	121.96
B (m)	16.816
T (m)	6.730
C_b []	0.65
l_e (m)	46.5
k_{yy} []	0.25

Table 2.2: S60 ship parameters

Figure 2.15: Non dimensional wave added resistance, ship: S175, $\alpha = 180^\circ$, $F_n = 0.3$

On the right graph, the orange figure represents the Lang and Mao model while the green one represents the Liu and Papanikolaou model. The Mittendorf model and the meta model are not represented. The blue figure represents another model which was not kept as it can only model head waves added resistance. Both models match pretty well the data for mid and long wave lengths. However, some deviation can be observed for short wave lengths. This might be due to the lack of information of the ship parameters. For example, the different drafts were not mentioned and had to be assumed. Furthermore, the data points were collected manually which is also a plausible source of error.

The last graph enables to compare all the models besides Mittendorf:

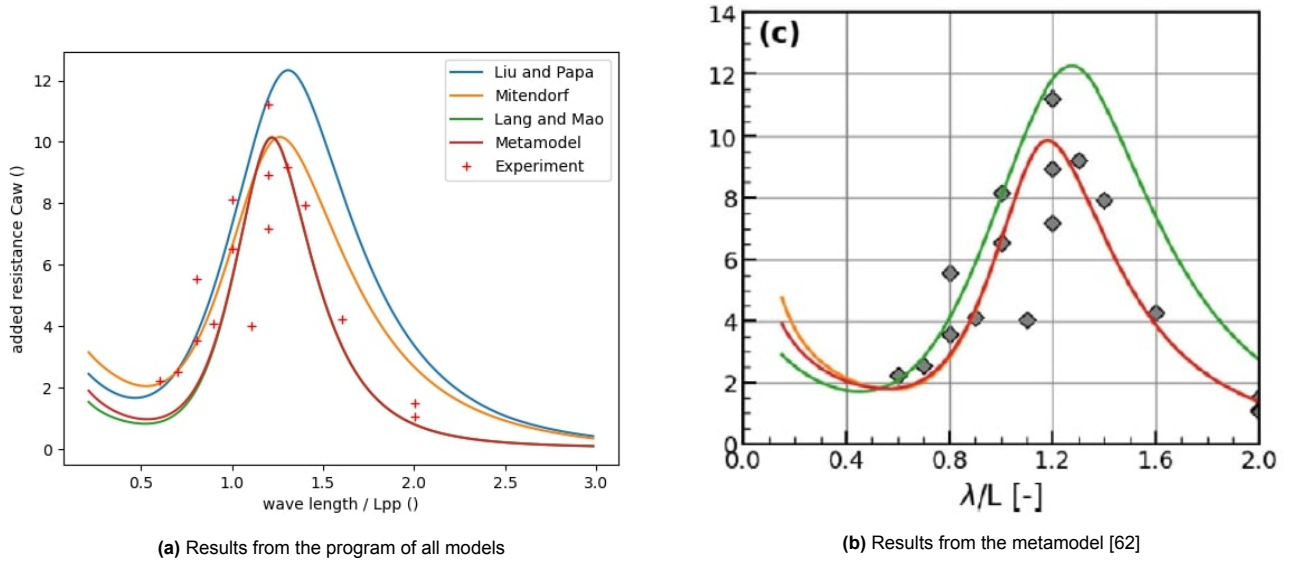


Figure 2.16: Non dimensional wave added resistance, ship: S60, $\alpha = 180^\circ$, $F_n = 0.283$

On the right graph, the green figure represents Liu and Papanikolaou, the orange one Lang and Mao and the red one represents the meta model. In this case, it follows mostly Lang and Mao. Likewise, both graphs are pretty similar. The meta model seems however to be lower for our implementation in the short wave length range. Overall, all models behave as expected in most cases. Only Mittendorf's model could not be completely verified. In fact the graphs from the article could not be used and data points were hardly accessible (3D figures for example). However, the program itself has been made available by the authors and was already retrieved by VPLP. Therefore, it is considered verified. They can now be implemented and adapted for VPLP's needs.

2.4. Implementation of the wave added resistance for VPLP Design

2.4.1. Irregular waves calculation

These models are all meant to be used for regular waves i.e monochromatic unidirectional waves. However, real sea conditions are almost never as such. This chapter will depict how to go from a monochromatic regular wave to a more realistic irregular wave spectrum.

In the literature, the mean wave added resistance in irregular waves is calculated as a linear superposition of the transfer function of added resistance in regular waves R_{AW}/ζ^2 and a directional wave spectrum E [60]:

$$R_{irr.wave} = 2 \int_0^{\frac{\pi}{2}} \int_0^{\infty} \frac{R_{AW}(\omega, \alpha, U) E(\omega, \alpha)}{\zeta^2} d\omega d\alpha \quad (2.29)$$

In practice, VPLP already has a package to compute wave spectra called Spectrum. It uses the equations from the 23rd ITTC report [56]. The inputs are a zero-crossing frequency T_z and a significant wave height H_s . The outputs are ranges of wave periods, amplitudes and angles. Before developing, it is important to define the different types of period that can be encountered when working with irregular wave sets:

- The peak period T_p corresponds to the wave with the highest energy. - The mean period T_m is the average period of all the waves in a time-series. - The zero-crossing period T_z (up or down crossing) is the period between two consecutive zeros of the function where the trend is similar (either increasing and going from negative to positive or the opposite).

The common spectrum used for this project is the JONSWAP spectrum (Joint North Sea Wave Observation Project) as it represents well the North Sea and North Atlantic regions, the latter being a common sailing area for the company's ships. With JONSWAP, it is also possible to switch from one type of period to another with a set of equations [56]. This spectrum also has a γ parameter which quantifies how developed the sea state is. A low γ means a developing sea state i.e the waves are just being generated by the wind and a high γ means the sea is already formed and the sea state is more regular. This parameter will not be chosen as equal to 3.3 (mean value) and will not be modified.

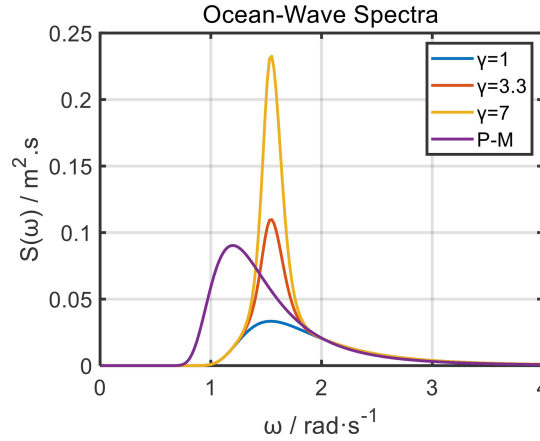


Figure 2.17: JONSWAP spectrum depending on γ

As shown above, a large γ implies a more formed sea state with a concentrated power in a small frequency range [59]. The P-M spectrum corresponds to the Pierson-Moskowitz spectrum, which is similar to JONSWAP but without the peak enhancement factor.

This JONSWAP spectrum is coupled with a directional spreading function which quantifies the angular spreading of waves. If $E(f)$ is the JONSWAP energy spectral density function, then the directional spectral density function will be defined as such [37]:

$$E(f, \theta) = E(f)D(f, \theta) \quad (2.30)$$

Where $D(f, \theta)$ is the angular spreading function. There are several different equations for this function. The one used for this project is one of the most common one and is already used for VPLP design's other projects: the cosine-squared formulation.

$$D(\theta) = \begin{cases} \frac{2}{\pi} \cos^2(\theta - \theta_0), & \text{for } (-\frac{\pi}{2} + \theta_0) < \theta < (\frac{\pi}{2} + \theta_0) \\ 0, & \text{otherwise} \end{cases} \quad (2.31)$$

where θ_0 is the mean wave direction in radians [37].

When using the Spectrum package of the company, the wave added resistance is then calculated for each generated set of wave height, period and angle of the output. The total wave added resistance is found by adding up all the results. For a chosen model, it yields:

$$R_{AW,irr} = \frac{\rho g B^2 \zeta_i^2}{L_{pp}} \sum_{i=1}^n C_{AW}(\alpha_i, t_i, H_{s,i}) \quad (2.32)$$

2.4.2. Implementation for VPLP Design's needs: PyWave package

One of the objectives of the thesis is to implement wave added resistance in a quick and simple way. Furthermore, the best model had to be found depending on the case scenario. The proposed solution was a program defined as a package called PyWave which will be depicted here. The package is divided in two classes, ShipParam and ShippingCondition which is a subclass of ShipParam. The former is composed of the main ship parameters that one can enter or through a specific file. The first function create_ship creates a ShipParam class from the given parameters. It also makes tests to verify that the values are physically meaningful (i.e a negative length between perpendiculars or a block coefficient larger than one are not possible). In some cases, if all parameters are not given the program will consider default values and warn the user. For example, if the normalized radius of gyration is not given, it will be assumed as equal to 0.25. This class also contains the four models mentioned above.

The subclass ShippingCondition also takes into account the ship speed and the wave data (wave angle, wave height and wave period). The first function creates a class and checks if the given values are within the range of all models. Furthermore, another boolean parameter is meant to have the results in monochromatic waves or with a spectral function. The speed unit is also an input as engineers and maritime companies usually work with nautical miles but the models require a speed in scientific units (i.e $m.s^{-1}$). A second function is therefore made to convert speeds with the required unit. Likewise, the following functions are made to calculate the Froude number in case it is not given and to convert incident wave angles in acceptable values (between 0° and 180°). Furthermore, the functions for the different types of period and the JONSWAP spectrum generation are coded.

Once all the ship parameters are checked and the class is created, the function choose_model will determine which model fits best the studied case. The methodology is inspired from the research on the meta-model [62] which is the only article that compares the different models depending on a various number of parameters such as the wave angle, the ship speed and the wave period. Furthermore, external data was provided to validate these results. This data was retrieved from CFD calculations to assess the power consumption and was made with data and parameters from a RoRo ship. It gives the fuel consumption depending on the speed and the weather conditions. However, it is important to note that in order to use it, some assumptions had to be made, especially in the propeller to engine system efficiencies and the figures can be pretty different from the models. In fact, it was used mostly to validate a trend rather than numerical values. This issue will be commented more thoroughly later in the report. Coming back to the previously mentioned article, it divides the wave angles, ship speed and wave length in three areas respectively. These are provided in the table below:

Wave angle (°)	Head waves	135-180°
	Beam waves	45-135°
	Following waves	0-45°
Wavelength/ L_{pp}	Short waves	0.1-0.3
	Mid waves	0.3-1
	Long waves	1-3
Froude number	Small F_r	0-0.1
	Medium F_r	0.1-0.25
	Large F_r	> 0.25

Table 2.3: Parameters ranges according to the meta-model study [62]

In the article, the mean squared error (MSE) is calculated to compare the models:

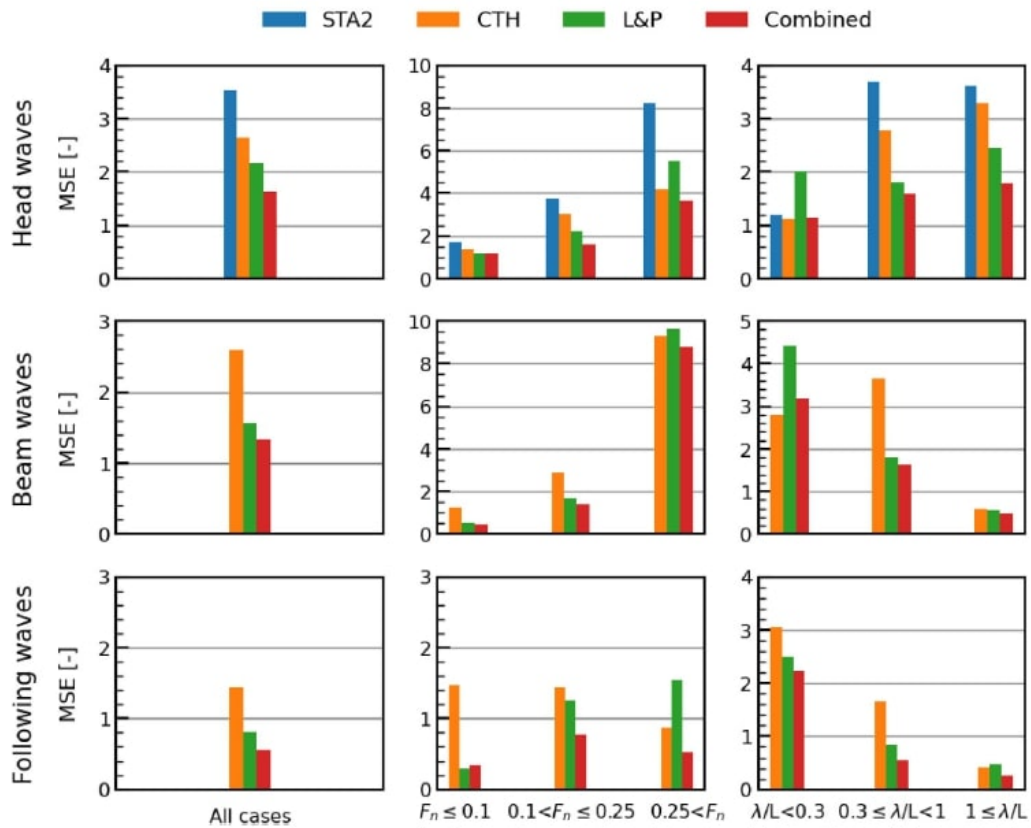


Figure 2.18: MSE comparisons of models

L& P stands for Liu and Papanikolaou, CTH is the Lang and Mao model and Combined is the meta-model. STA2 was not kept as it does not calculate the wave added resistance for non head waves. These figures helped establish the optimized range for each model.

For each combination of speed, wavelength and incident wave angle, the best model is given. Furthermore, the article also compares the results depending on the ship type. These results are compiled in a second file included in the package:

model_choice_parameters2.json. In this file, the choices are presented as a decision tree in which one (or multiple) appropriate model is given at the end of each branch.

This file is divided in two parts. In the first part, the different validation ranges of the four models in terms of ship parameters are presented. The code below shows how it is presented for the Lang and Mao model:

```

1  "Lang and Mao": {
2  "Name": "Lang and Mao",
3  "Ref_Article": "Lang and Mao 2021",
4  "Lpp_min": 90,
5  "Lpp_max": 355,
6  "B/L_min": 0.139,
7  "B/L_max": 0.184,
8  "T/B_min": 0.227,
9  "T/B_max": 0.401,
10 "Cb_min": 0.54,
11 "Cb_max": 0.829,
12 "Fn_min": 0,
13 "Fn_max": 0.3
14 },

```

If the chosen ship fits a certain model, the latter will be given "a point" and kept for further tests. Then, the code will use the wave parameters given as an input to find the best models. Likewise, these ones will receive an extra point. Eventually, the program will check the ship type and give an extra point as

well. Eventually, the model which passed the highest amount of tests will be proposed to the user. The example below might enlighten the way it is used. Let us consider a general cargo with the following parameters:

L_{pp} (m)	97.311
B (m)	20
T (m)	4.7
C_b []	0.668
l_e (m)	42.65
l_r (m)	15.45
k_{yy} []	0.25

Table 2.4: Example ship parameters

For this ship with relatively "normal" dimensions, it is in the range of all models. If we take the following conditions: $F_r = 0.08$, $\alpha = 160$ and $\frac{\lambda}{L_{pp}} = 0.25$. The conditions match a head wave, short wave and small Froude scenario. Therefore, `choose_model` will look for that area in the `model_choice_parameters2.json` file. The structure of a segment of this file is presented below.

```

1   "Head waves": {
2     "alpha_min": 135,
3     "alpha_max": 180,
4     "short waves": {
5       "lambda_min": 0.1,
6       "lambda_max": 0.3,
7       "small Froude": {
8         "fn_min": 0,
9         "fn_max": 0.1,
10      "models": [
11        "Metamodel"
12      ]
13    },
14    "medium Froude": {
15      "fn_min": 0.1,
16      "fn_max": 0.25,
17      "models": [
18        "Metamodel",
19        "Liu and Papanikolaou"
20      ]
21    },
22    "large Froude": {
23      "fn_min": 0.25,
24      "fn_max": 10,
25      "models": [
26        "Liu and Papanikolaou"
27      ]
28    }
29  },

```

As one can see above, the best model in that case is the meta-model. It will be chosen by the program to calculate the wave added resistance. Sometimes, more than one model can be chosen. In that case, the model is chosen in this order: Liu and Papanikolaou, Lang and Mao, Meta-model and Mittendorf.

The head waves section of this file is provided below as a table:

Head waves (135°-180°)	Short waves (0.1-0.3)	Small F_r (0-0.1)	Metamodel
		Medium F_r (0.1-0.25)	Metamodel and L&P
		Large F_r (>0.25)	L&P
	Mid waves (0.3-1)	Small F_r (0-0.1)	Metamodel and L&P
		Medium F_r (0.1-0.25)	All models
		Large F_r (>0.25)	Metamodel and L&P
	Long waves (1-3)	Small F_r (0-0.1)	Lang and Mao
		Medium F_r (0.1-0.25)	Lang and Mao
		Large F_r (>0.25)	Lang and Mao

Table 2.5: Head waves section of the table in model_choice_parameters2.json

The table is then completed with the appropriate model depending on the ship type:

Head waves (135°-180°)	Tanker	L&P, Metamodel and Mittendorf
	Liquefied gas	L&P, Metamodel and Mittendorf
	Bulk carrier	L&P, Metamodel and Mittendorf
	General cargo	Lang and Mao and Metamodel
	Container ship	L&P, Mittendorf and Metamodel
	Roro	Lang and Mao and Metamodel
	Ferry	Lang and Mao and Metamodel

Table 2.6: Model per ship type for head waves

These two tables are then repeated for beam waves and following waves. Figures in the subsection below highlight the results and the way the optimized model is chosen.

2.4.3. Results and comparisons

The external data provided wave added resistance results for a RoRo ship with the following values for the main parameters:

- Wave heading: from 0° to 180° with a step of 15° - Significant wave height: from 0m to 10m with a step of 1.5m - Wave period (in s): 2.0, 4.0, 5.5, 7.5, 9.0, 10.5, 13.0, 16.2 - Ship speed: from 4kn to 23kn with a step of 1kn (except 6, 21 and 22kn)

Therefore, the resistance was calculated for these values with all four models to compare. This yields 1560 different graphs with four models (plus and optimized model chosen out of these four) and the external data calculated by CFD. The ship used for to generate this data is a Roro and has the following dimensions:

L_{pp} (m)	154.265
B (m)	22.83
T (m)	5.384
C_b []	0.61
l_e (m)	51.7
l_r (m)	21.36
k_{yy} []	0.25

Table 2.7: External data ship dimensions

As a side note, most values were given but the length of run and length of entrance were estimated which can lead to some error. The periods and the L_{pp} give the following values for $\frac{\lambda}{L_{pp}}$:

Period [s]	Wavelength [m]	$\frac{\lambda}{L_{pp}}$ []
2	6.24	0.04
4	25.0	0.16
5.5	47.23	0.31
7.5	87.8	0.57
9	126.47	0.82
10.5	172.13	1.12
13	263.86	1.71
16.2	409.75	2.67

Table 2.8: Values of period/wavelength from external data

A first look at this table shows that the first value is relatively low ($0.04 < 0.1$). Therefore, we can assume that the resistance given by the models will probably diverge and should not be taken into account. Therefore, only the second value fits in the short wave category. The following three fall in the medium wave category (although the first one is at the edge of the range) while the last three are long waves.

Eventually, with high waves, the number of points decreases. In fact, when waves get higher, it becomes impossible to have a short period. In that case, the wave becomes too steep and starts to break. The problem is not linear anymore and is out of the scope of this masters thesis. The examples below will rather focus on smaller waves (between 0 and 3m) to show figures with all sizes of wavelengths. All the figures were generated by Jupyter Notebook and are presented with the period in seconds as the x-axis and the wave added resistance in kN as the y-axis.



Figure 2.19: Wave added resistance, V=14kn, head waves, all models plus external data

In the figure above, one can see how the models diverge in 0 especially the Lang and Mao model when the data converges towards 0. This confirms that the first point is not relevant for our study. Here, 14kn corresponds to a Froude number of 0.185 which places our simulation in the medium Froude range. The graph below shows the same figures without the first point:



Figure 2.20: Wave added resistance, V=14kn, head waves, all models plus external data without first point

In this case, the Lang and Mao model seems to be the closest to the data in the medium and long wavelength. Furthermore, its peak is obtained for the same period (9s) whereas the peak of both Liu and Papanikolaou and Mittendorf models come before (7.5s) Therefore, it should be chosen as the best model in this case scenario.

Results sorted by Speed_kts

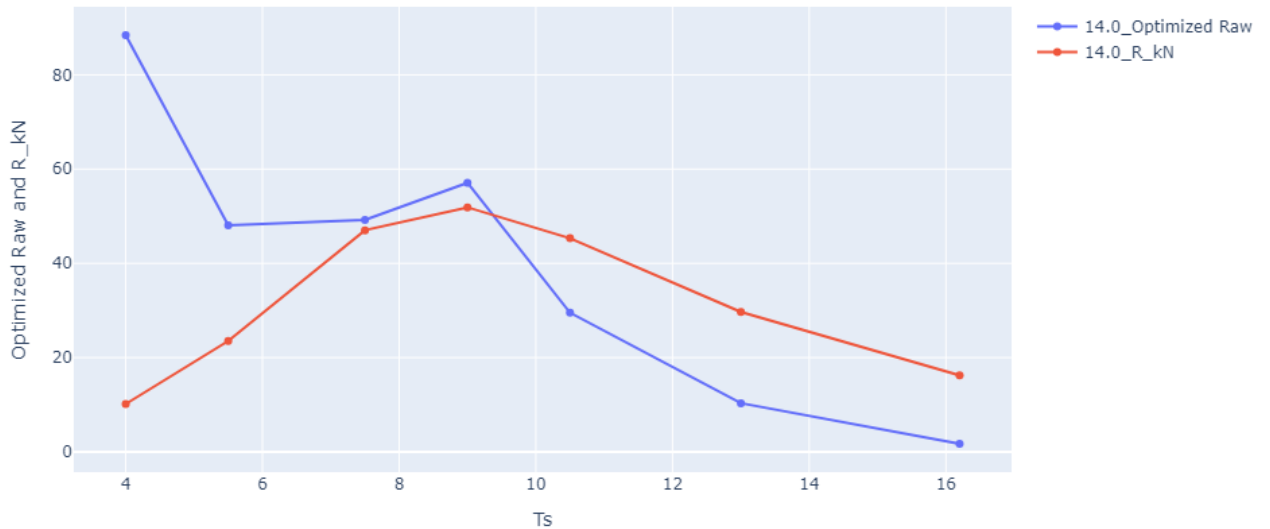


Figure 2.21: Wave added resistance, $V=14\text{kn}$, head waves, optimized model plus external data without first point

Indeed, the optimized model is Lang and Mao in this configuration as shown in the plot above. The `model_choice_parameters2.json` file mentioned in the section above was created by repeating this operation with all the different configurations and finding the best option.

The simulations also confirm the resistance behaviour when the wave angle shifts towards beam waves:

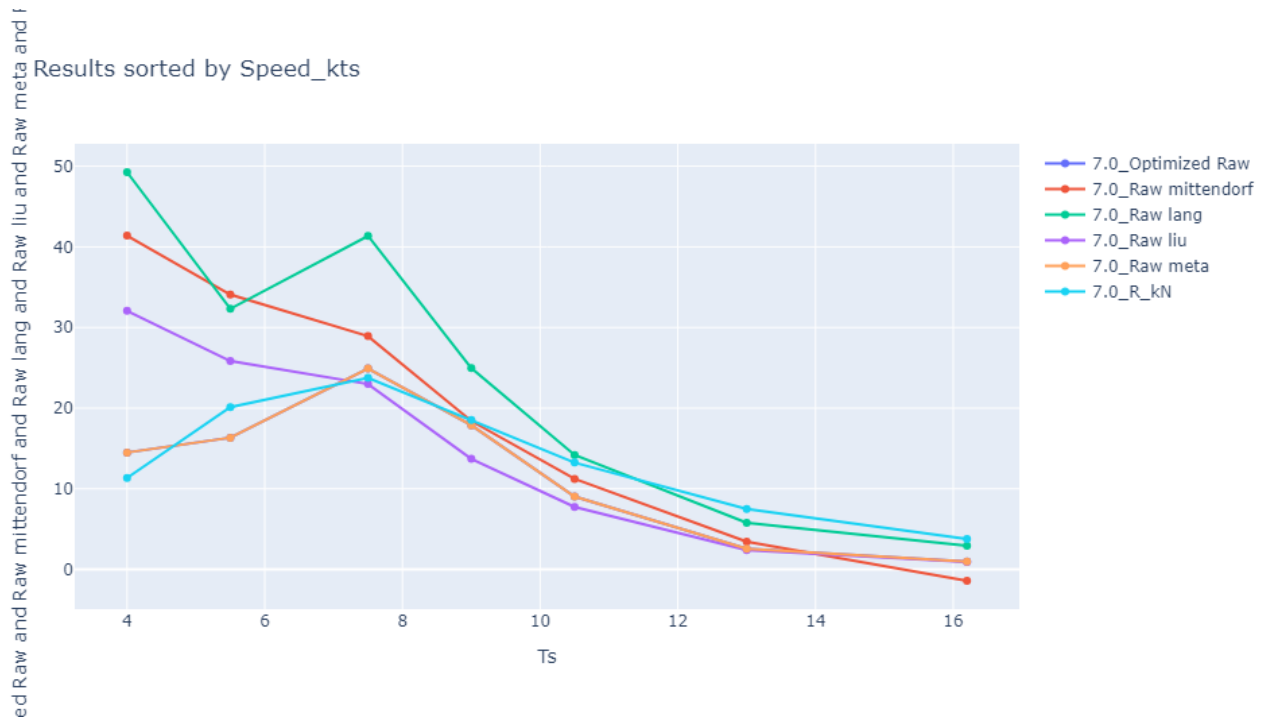


Figure 2.22: Wave added resistance, $V=7kn$, $\alpha = 135$, optimized model plus external data without first point

The peak of the resistance also shifts towards shorter wavelengths ($T_s = 7.5s$). In this case, the optimized model is the meta model, and both figures coincide.

In low speed following wave scenario, some models take into account a negative wave resistance which comes from the fact that waves are faster than the ship and "push" it forward:

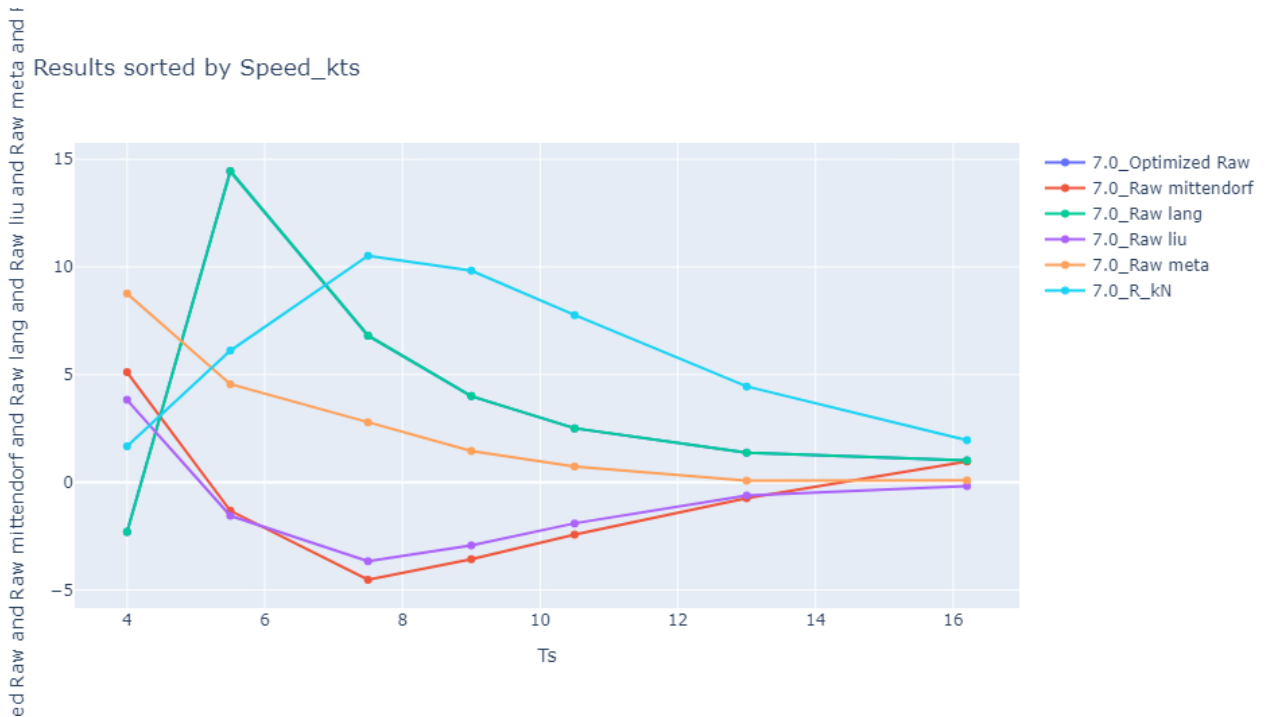


Figure 2.23: Wave added resistance, $V=7kn$, $\alpha = 0$, all models plus external data without first point

Liu and Papanikolaou and Mittendorf are the only ones to give a negative resistance.

Overall, it seems that Mittendorf is the least accurate model so far Lang and Mao's model and the metamodel are the most popular. Two factors could explain this behavior. The model created by M. Mittendorf has a special focus on the Block coefficient and is improved compared to Liu and Papanikolaou for $C_b > 0.7$ [38]. The example ship here has a C_b of 0.6. Another factor is the ship type. The example ship here is a Roro which seems to favor Lang and Mao's model and the metamodel. So far, the program has been adapted for RoRo ships by using the aforementioned external data and gives the most accurate wave added resistance model for such ship. For a more thorough investigation, it could be interesting to repeat the operation with different ship types.

2.4.4. Limits and suggestions

Obviously, the values of the figures are quite far from the data. As mentioned before, the external data was mostly fuel/power consumption depending on the weather conditions and the ship's speed. Many assumptions had to be made by the team concerning the engine/propeller properties plus the overall efficiency of the propelling system. From this, the calm water resistance was found and the difference between this result and the data gave the wave added resistance. The main limit here is the validation process.

In fact, this data combined with the information found in the article were used to give a first educated guess on the model choice. Further validation process with onboard data from VPLP's ships are planned and should be executed to adjust the PyWave package. The benefit of this program is that the `model_choice_parameters2.json` file is very easy to modify once more relevant data will be accessible and the programs can quickly calculate wave added resistance for a great number of case scenario (1560 for this set of data).

To remain consistent, VPLP intends to choose one model for a specific ship/journey combination and stick with it instead of using a different one for each point. So far, the program chooses a model only for the second option. Therefore, the plan is to run numerous simulations for entire trips and choose the model that provides the most consistent average wave resistance. This can quite easily be done and could be an interesting topic for further investigation.

3

Routing software optimization

3.1. Software Presentation

3.1.1. TZStat routing software

TZStats is the routing software used by VPLP. It was developed for wind assisted ships in order to optimize a fuel consumption for a specific journey. It can also run a certain amount of journeys at the same time which makes it useful for statistical studies and performance predictions. The inputs are the following:

- Date of departure
- Date of arrival (this gives the average ship speed during the journey)
- A csv file with a reference route with a few coordinates from which the software generates an optimized route
- The weather data files corresponding to the geographical area and the dates of the trips.
- A csv file corresponding to the "cost" values (or more generally the parameter to optimize) depending on the ship's speed and the meteorological conditions. In the example files, there were mostly fuel consumption in $kg.h^{-1}$. The use of sail or not is also taken into account.
- The space step used by the software (a few tests had to be done to assess the impact of this input on the results and will be further developed).
- The number of journeys and the gap between each departure.

Other optional inputs are possible and will be depicted if necessary.

The outputs will be two new csv files and a third csv file will be modified:

- The first file will contain all the information of the journey at every moment of the journey (the amount of points i.e the number of lines will depend on the space step).
- The second file will contain the average values of different parameters during the journey.
- Running a journey will also add a line to a third csv file which contains the average values of different parameters for all the trips (each line corresponds to a trip).

The weather data files are selected from the ECMWF. The space resolution is set to 0.5° .

3.1.2. Specific use for VPLP Design

VPLP Design uses this software in order to have average values of fuel consumption for a specific journey. The method is the following:

The team runs a certain amount of journeys with a week interval between each departure during a whole year. From these simulations, they retrieve all the data and can show the average improvements on fuel consumption. In this study, the journey was between Saint-Nazaire, France and Mobile, Alabama. The ship sails for about two weeks and the simulation was made with the weather data from the year 2018. Therefore for each test, we would retrieve 51 simulations.

The reference route coordinates are given below.

Lat	Lon	Rail	CanUseSail	Date	StepSide
47.21	-2.225				0
47.07807	-2.54773	1			0
27.35	-78.45				0
26.8	-79.1	1			0
25.73657	-79.70856	1			0
24.711	-80.4	1			0
24.38	-81.38	1			0
24.364	-82.12069	1			0
24.6872	-82.41806	1			0
30.00989	-88.01147				0
30.19677	-88.05972	1			0

Figure 3.1: coordinates of the reference route

The map below shows the shortest route and the reference points:

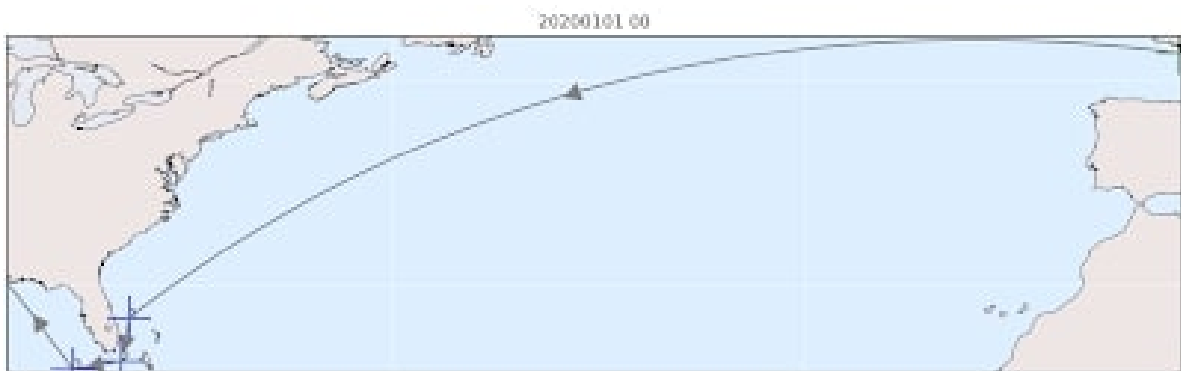


Figure 3.2: Reference route between Saint-Nazaire and Mobile

Onboard the studied ship, different wings have been used. This study also enables to have an idea of the most efficient wing for this trip and ship and the one to recommend for potential customers. However, this mission was out of the scope of the research project. It is important to keep in mind that the

goal was to develop tools to make statistical studies rather than make such studies.

The trip's characteristics are depicted below:

Parameters	Values
Travel time	13 days 17h 37min 25s
Orthodromic distance	4449.90 nm
Average speed	13.5 kn

3.2. Influence of space step

3.2.1. Method for assessing the influence of space step

The space step of the software can be modified on a range from 0.01° to 5° . Our first theory was that the output values would tend to converge if the step decreases (i.e the accuracy increase) until it reaches the weather data's step (0.5°). From that accuracy, the values should not change as the software would choose the same weather values. Therefore, a certain number of tests were made with different space steps. Naturally, the computational time tends to increase with the accuracy and this phenomenon will be mentioned later. However, for very short space steps (below 0.1°) and some trips, TZStats would sometimes crash.

In order to asses its influence, simulations were done for space steps ranging from 0.1° to 5° with the same trips and during the same year as mentioned previously. The data are shown below and represent a "cost" depending on the departure week.

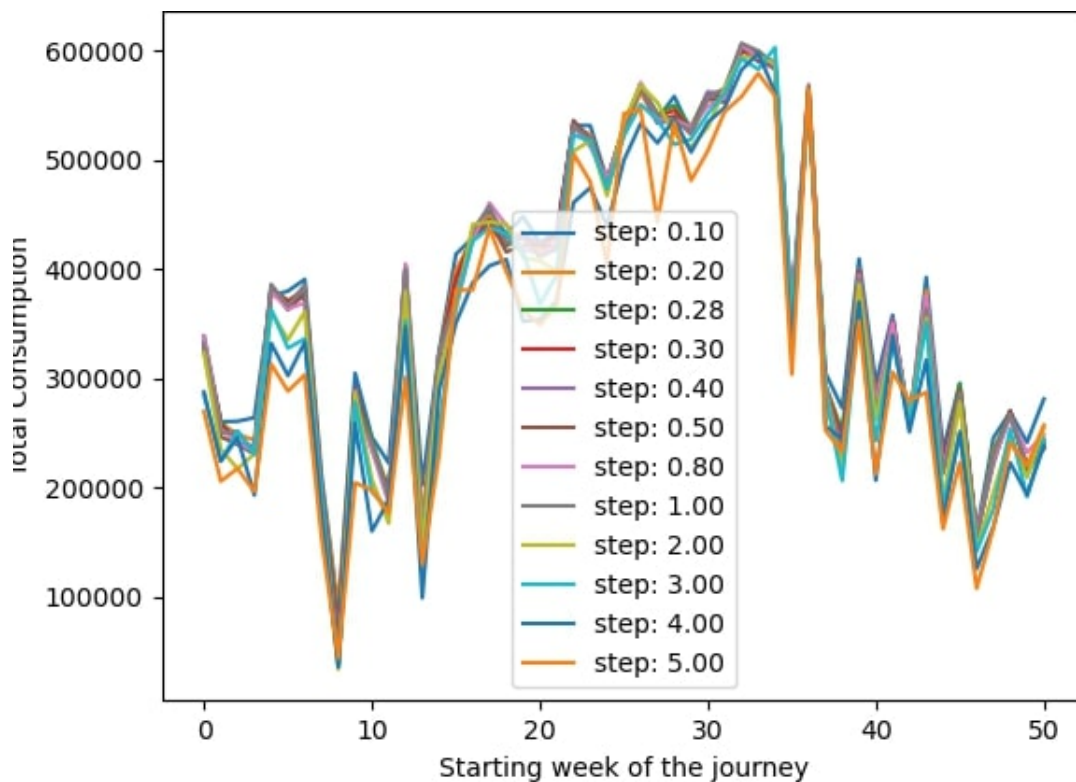


Figure 3.3: Total consumption for each trip

The results follow the same trend for each space step used. For your information, there are only 51 journeys as a 52nd one would arrive at the beginning of the next year and would thus exceed the weather data file.

If we zoom in on some specific trips, one can find major differences.

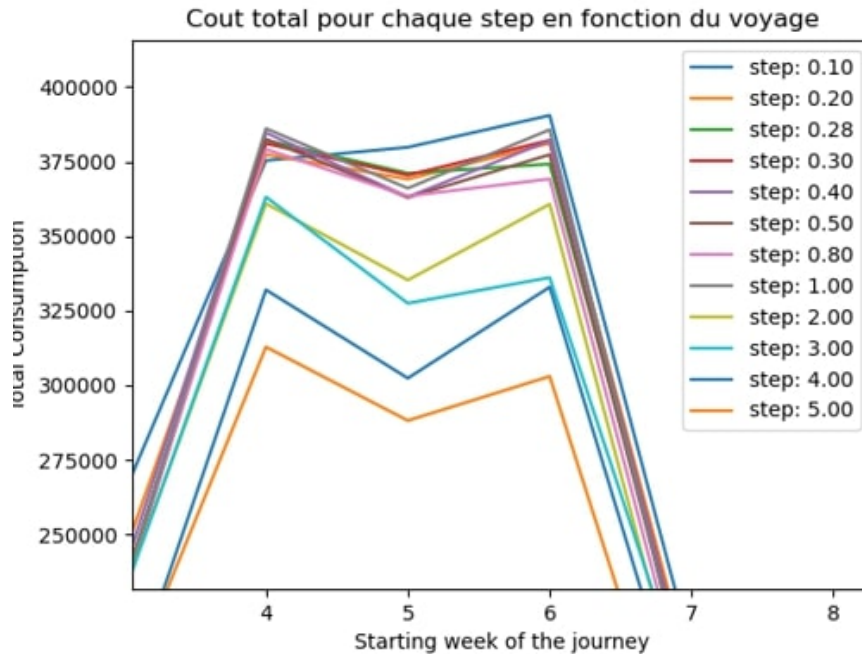


Figure 3.4: Total consumption for the trips 4,5 and 6

For the fifth departure, that would mean leaving on the first day of the fifth week of the year, the total fuel consumption with a space step of 0.1° is around 380 000 while the value is close to 287 000 which makes a difference of around 25%. This difference is definitely not negligible. This trip reaches a maximum and if we take the average cost of all the trips for each space step, the gap between the smallest and largest averages is about 13.5%.

Once these differences were made, a question arose: Do the results converge when the space step decreases?

From the average cost for each space step, a normalized mean cost for each space step is calculated:

$$C_{norm} = \frac{C - c_{min}}{C_{max} - C_{min}} \quad (3.1)$$

The results are presented below:

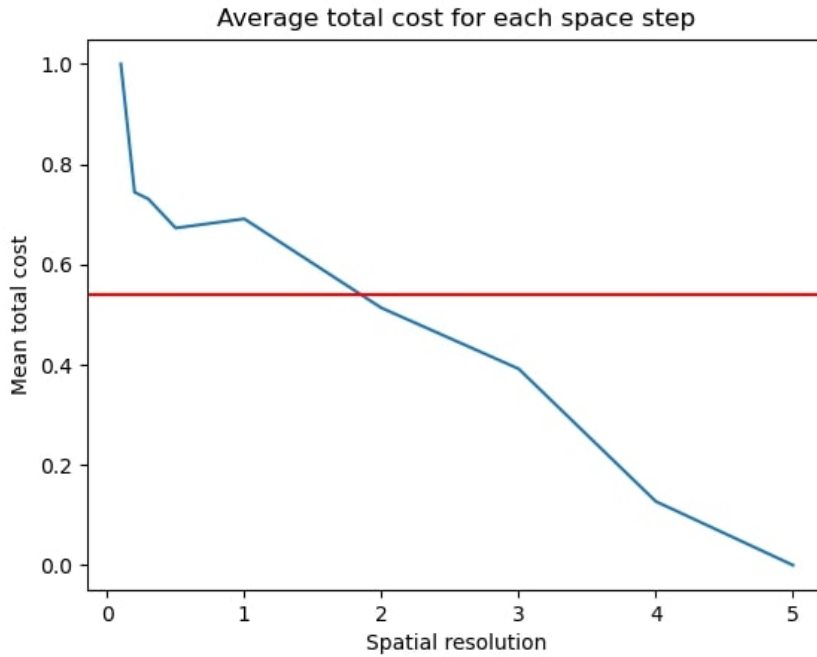


Figure 3.5: Normalized mean cost

The red line represents the average. One can observe a certain convergence where the results are pretty similar for space steps ranging from 0.2° to 1° . However, the results diverge when the space step becomes even smaller. In terms of cost, the results are more pessimistic when the accuracy increases but it is difficult to assess how reliable these figures are. These results are pretty similar with different ships and different sets of sails.

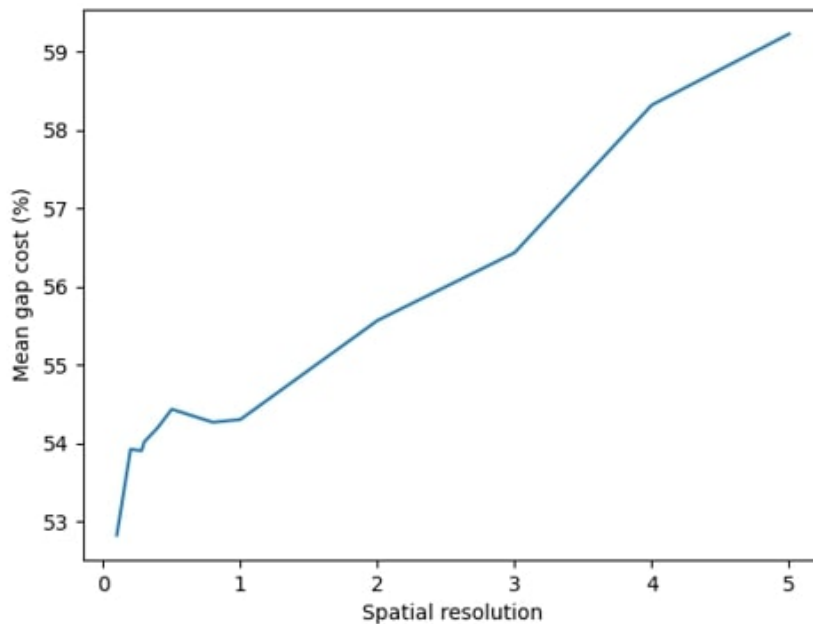


Figure 3.6: Mean consumption gap between a ship with sails and one without

The figure above was obtained with the following equation:

$$Gap = \frac{C_{ref} - C_{sail}}{C_{ref}} * 100 \quad (3.2)$$

Once again one can see a sort of plateau around 0.5° but the mean consumption gap between a ship using sails and one that is not keeps on decreasing.

However, for a reverse trip (between Mobile and Saint-Nazaire), this space step influence is almost non-existent. Furthermore, as TZStats is made by another company, the code is inaccessible and it is complicated to understand how it works without seeing it. That is why we contacted the company and exchanged with them on these topics. It enabled them to fix their program and adjust to VPLP's needs. Overall, the software now converges and the space resolution will be set to 0.5°.

3.2.2. Impact on computational time

Naturally, the computational time increases when the space step decreases. Running the tests can take a few minutes with a step of 4° or 5° (and generally any value above 1°) but the delay increases quickly below. For a chosen space step of 0.5°, running 51 trips takes approximately one hour. Below 0.1°, it was common for the software to crash.

This computational time is not "huge" in regard to some other programs but it adds up with the ones from the other studies. In order to improve this duration, the software can run in parallel computing (batch) to improve its computational time.

4

Optimized tool for metoceanic analysis

4.1. Depiction of statistical analysis

Another requirement for the company is to know the general sea conditions a ship might encounter on a specific journey. Therefore, statistical weather studies are required. VPLP Design had already developed tools for the wind conditions however, the wave conditions and the wind/wave combinations had to be added to this tool.

4.1.1. Ships performance prediction

A velocity prediction program (VPP) is used to determine the performance of sailing ships for different wind speeds and wind directions. Most VPP are iterative programs which require a certain amount of initial parameter to start with. When weather data statistics are implemented, they can be used to improve mathematical models and in our case assess the wave added resistance during a journey which increases the accuracy of the VPP. This methodology helps improve the engine to propeller matching study or the routing simulations. The scheme below shows how the iteration works.

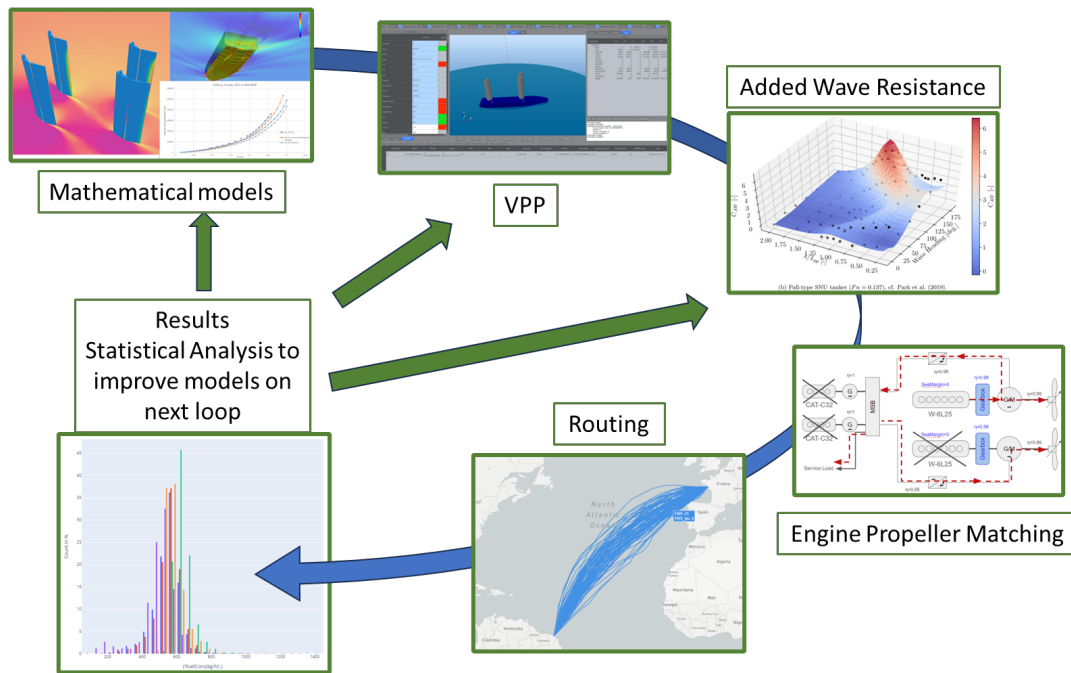


Figure 4.1: Performance prediction process

Sailing ships' VPP is usually a 3D polar Matrix composed of wind direction, wind speed and ship speed. In the case of sailing yachts, the speed is usually the parameter that is optimized. However for cargo ships, the speed is usually a constant and the program tries to optimize the fuel consumption for a specific route.

4.1.2. Particularities for WASP

While conventional ship are only propelled by an engine (usually Diesel engine), saving fuel is usually done by decreasing the speed [29] or sailing on the shortest possible route (i.e orthodromic route). If we consider a constant speed, ships equipped with WASP must try to maximize the use of this system to optimize their fuel consumption. In that case, the shortest route is not always the best option. The routing system must find the best possible winds to optimize the use of sails while ensuring a constant speed and especially while making sure the ship arrives at the predicted date and time. This calls for a VPP which can generate accurate polar matrices. In that case, correctly assessing the impact of the wave added resistance becomes even more crucial.

4.1.3. From 3D to 6D study

As explained previously, waves which have an impact on a ship's resistance are usually generated by wind. The routing system must then find a trade-off between windy conditions and an agitated sea. When adding wave effects, the polar matrices developed by the VPP become more complex, growing from 3D to 6D. The three new dimensions are the following:

- wave peak period
- wave direction
- significant wave height

The polar matrices can now give the fuel consumption for each wind/wave/ship speed combination. One obvious offset is the increase in size of the output csv files which then increases the computational time of the different programs using it such as the routing software. As an order of magnitude, one file can have more than a million lines and weight a few Gigabytes. Some solutions to this issue will be addressed in the next section.

4.2. Metoceanic tool for a specific journey

4.2.1. PyRoute package optimization

PyRoute is a package developed by VPLP for weather studies. Among other things, it enables to retrieve data from the Copernicus program and show the most commonly encountered weather for each of the company's ship. So far, it has been mostly used to study wind state. However, the wave added resistance required to also study the sea state. From this package and new programs, it is now possible to easily study the frequency of wind/wave parameters for a chosen route at any time between the first data records and the most recent ones.

4.2.2. From a route to desired wind/wave components

The first step is to define the time and location of the study. Therefore, the program (`tz_to_route.py`) first requires a specific year and a journey from which the studied area will be defined. The latter will be generated from the most south-western and north-eastern coordinates the ship travels to. All the wanted data within this rectangle will be downloaded plus a certain margin. The default margin used by the company is 0.25. For example, the Avenir ship is supposed to sail along the Italian coasts in the Mediterranean sea and work as a rescue vessel for migrants sailing across the sea. Its expected journey is shown below:



Figure 4.2: Itinerary of the Avenir ship

The coordinates are stored in a csv file in the same format as for TZStats which is mentioned in the previous chapter. Furthermore, one can add a step size which will determine the amount of points. A small step size will add more points and thus more data but implies a larger computational time. Once this rectangular area is generated, all the required data is downloaded for the whole year as a GRIB file. The studied years during our tests were mostly 2018, 2019, 2020 and 2021. Eventually, the data are the following:

- 10m u component of wind
- 10m v component of wind

These two components were already downloaded before and enable to calculate the true wind speed and true wind direction (0° corresponds to the wind flowing from the North to the South). The u and v components correspond to the speed vectors in the West-East direction and the South-North direction respectively. The true wind angle is calculated from the true wind direction and the course over ground (positive when starboard tack).

Among others, the new program also downloads the following data:

- mean wave direction: this is used along with the course over ground to calculate the mean wave angle
- peak wave period
- significant height of combined wind waves and swell

Other parameters can be interesting but they will not be downloaded in this case:

- significant height of total swell
- significant height of wind waves

Once this data is collected, the next step consists in retrieving the data a ship will encounter during a specific journey. The next program (`route_to_matrix.py`) requires the previously downloaded GRIB file, a route, the departure date (included in the year of the GRIB file) and the ship speed as inputs. Just as TZStats, it is possible to simulate more than one trip all along the year therefore multiplying the amount of data.

As with the TZStats program, the output will be a csv file in the form of polars with the wind and wave parameters. The last column will show the relative amount of time the ship spent in these conditions for every possible combination. That way, one can observe what are the most frequent wind/wave conditions encountered during a specific journey. However, it is required to find a suitable range and step for each parameter. So far, it has been done manually in the last program (`matrix_to_stat.py`). A more thorough optimization is mentioned in the next improvement section.

4.2.3. Examples and results

Canopée is supposed to sail across the Atlantic Ocean from Saint-Nazaire, France to Kourou, French Guiana from where the ESA rockets will be launched. In this case, it is interesting to note the different conditions encountered between one way and the return:

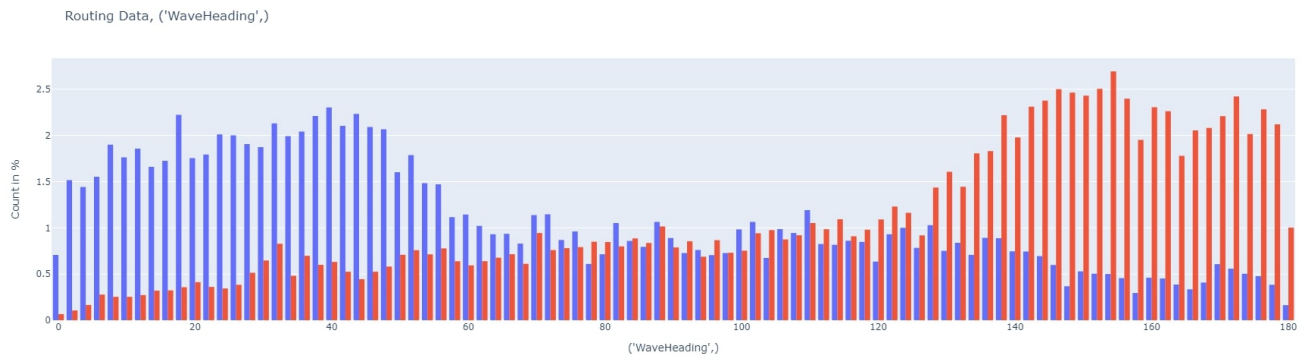


Figure 4.3: Encountered wave angle depending on the journey

The blue bars represent the percentage of encounter for each wave heading for a trip Saint-Nazaire/Kourou while the red bars are for Kourou/Saint-Nazaire. One can clearly see that the waves are pretty regular in this region which means the encountered waves in one way will be exactly the opposite in the other way.

On the other hand, the wave period and significant wave height will be relatively similar no matter the trip.

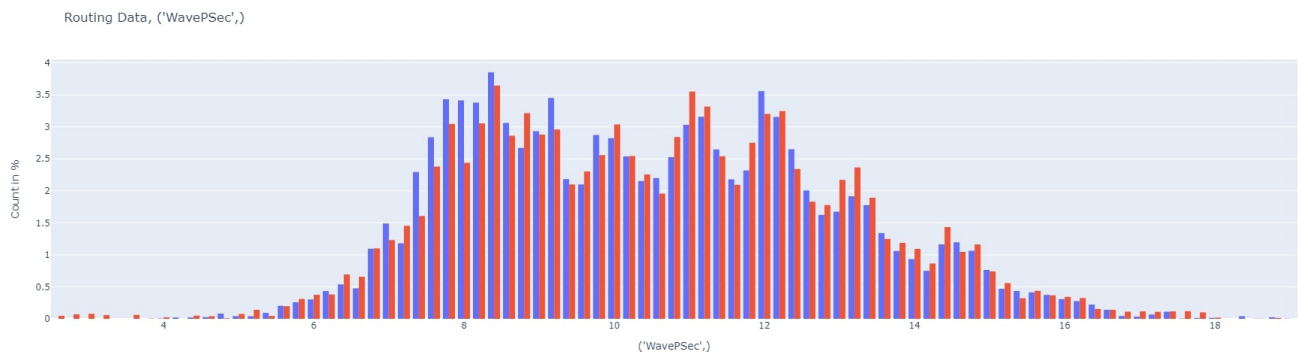


Figure 4.4: Encountered wave period depending on the journey

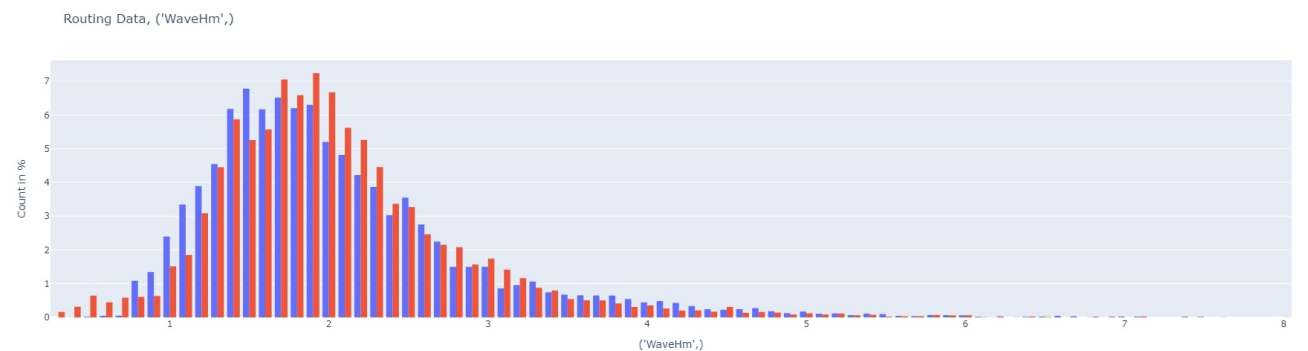


Figure 4.5: Encountered significant wave height depending on the journey

On the figure above, one can see that most of the encountered waves have a height between 1 to 3m and very few waves reach 4m or more. The team can therefore focus mostly on this range of waves to assess the performance of the ship on this itinerary. Likewise, the ship will mostly encounter head or

following waves depending on the way but fewer beam waves. Once again these different ranges can also be used for a performance prediction study.

4.2.4. Suggestions for improvement

As mentioned before, this statistical analysis tends to have large computational times.

One option to reduce the computational time was to use smaller GRIB files instead of one large one so the program would search the required values in a shorter list each time. In reality, GRIB files are usually only downloaded once, so it would probably only be longer on the first try. Furthermore, downloading a large file implies having a lot of data that will not be used.



Figure 4.6: Saint-Nazaire/Mobile journey

For example, if the route above is chosen as an input, the downloaded GRIB file will correspond to the data of all the coordinates in the image above. The program would have to go through data corresponding to coordinates near the coasts of Portugal or near the North-American Eastern coast which is not at all close to the ship's trajectory. With smaller files, the program would not have to go through such data and find the coordinates faster. A test has been done with files representing squares with the following dimensions: $5^{\circ} \times 5^{\circ}$. The computational time was compared with the original program's time. As a reminder, they both take a route, a departure date and a ship's speed as an input and return a matrix with all the wind/wave parameters encountered by a ship. The time was measured with snakeviz:

- 147s (2min 27s) in total for the program using just one file - 561s (9min 21s) in total for the program using multiple files

Obviously the results are quite the opposite as predicted. When looking in to the details, the method enables to gain some time on the research part, however it is completely overwhelmed by the time needed to open each file. Furthermore, a specific class is made whenever a file is opened and it takes even more time to generate it.

Another option that VPLP will look at will be working on the amount of values and the range for each of them. This is done in the last program which return frequency statistics from the data matrix. As an example, the following range was used in the examples:

```

1 tws_range = [0, 2.5, 5, 6, 7, 8, 10, 12.5, 15, 20]
2 hs_range = [0, 0.3, 0.5, 0.8, 1, 1.3, 1.5, 2, 2.5, 3]
3 tp_range = [3, 3.5, 4, 4.5, 5, 5.5, 6, 6.5, 7, 8, 9, 10]
4 twa_range = [-180, -165, -150, -135, -120, -105, -90, -45, -15, 0, 15, 45, 90, 105, 120, 135,
               150, 165, 180]
5 wh_range = [-180, -165, -150, -135, -120, -105, -90, -60, -45, -15, 0, 15, 45, 60, 90, 105,
               120, 135, 150, 165, 180]

```

Where tws is the true wind speed, hs the significant wave height, tp the peak period, twa the true wind angle and wh the wave heading.

Yet in some cases, the wind/wave parameters are concentrated in a closer range during most part of the journey.

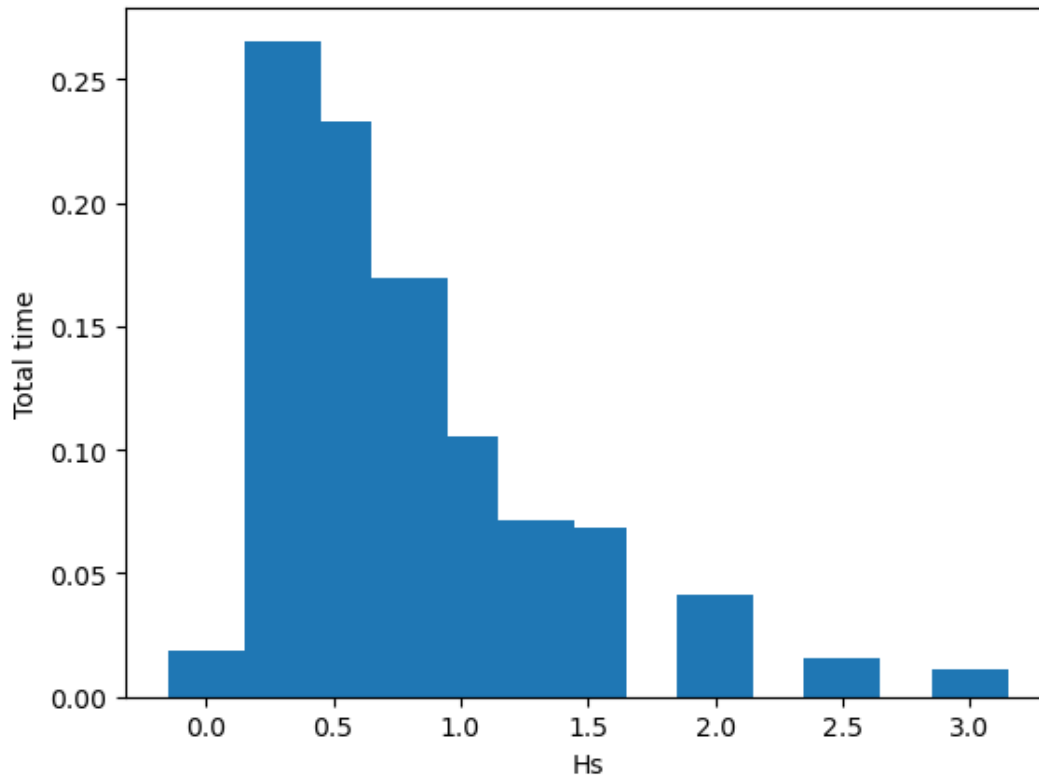


Figure 4.7: Simulation of encountered Hs during a journey of Avenir ship (2020)

In the graph above, we can see that around 75% of the encountered waves were actually between 0.3 and 1m high while around 5 % of them only were above 2.5m for the Avenir ship in the Mediterranean sea. In that case, it could be interesting to have a smaller range and less studied values for the significant wave height. Likewise, this study could be done for every parameter to optimize the number of possible values and thus the number of lines and computational time. Overall, it may help to focus on specific ranges to reduce the polar matrices used as input for the performance prediction program.

5

Conclusion

5.1. Final tool

5.1.1. Wave added resistance implementation

The main topic of this masters thesis was about implementing the wave added resistance applied on a ship. The solution we came up with is a python package called PyWave.

The company required a fast, reliable and semi-empirical way for deriving it. Furthermore, the program must be able to calculate the wave added resistance in every situation.

The package uses four of the latest semi-empirical methods published in the scientific literature. A wave spectrum was also added to compute the resistance of a set of irregular waves instead of a theoretical regular, monochromatic wave. With the help of these articles and the use of external data, a most suitable model is picked by the program for each case scenario. The program can now easily and quickly compute an accurate resistance and only requires simple ship dimensions. Furthermore, it can take as input a large range of ships and a large range of waves.

5.1.2. Routing software optimization

TZStats was the new routing software used by the company. It is to be used with ships equipped with WASP and tries to optimize its fuel consumption for a constant speed. When most ships try to sail on the shortest route, TZStats finds a trade-off between the distance and a windy route to optimize the use of the WASP and decrease the ship's CO2 emissions. Its inputs were 3D polar matrices with the fuel consumption depending on the ship speed and the wind parameters (wind angle and wind speed). However, it did not take into account the wave added resistance which can add up to 20% resistance compared to the calm water resistance. Furthermore, wind and waves are strongly correlated as the former generate the latter. With PyWave, the wave added resistance can now be calculated and its impact on the total fuel consumption is implemented. The polar matrices can now be in six dimensions with the significant wave height, the wave period and the wave angle.

5.1.3. Statistical analysis program

VPLP often makes statistical weather analysis on the trips the future ships will make to improve their models.

A python package from the company could retrieve wind parameters to check and study the occurrences of certain types of wind conditions along a route.

This program was improved to retrieve wave data as well. It can retrieve significant wave heights, wave directions and wave peak periods from a Copernicus database along a trajectory and plot frequency graphs to perform statistical study on the sea conditions.

5.1.4. Tool combination for an overall performance prediction

This thesis was made within the performance team of VPLP. The main goal is to predict and/or improve the performance of a ship. In the context of global warming, the company must be able to assess the CO₂ emissions of its ships. The wave added resistance may imply an extra fuel consumption thus more CO₂, therefore it must be computed accurately. Integrating it in a routing software enables to evaluate this increase in fuel consumption during a journey and makes the software more relevant when it comes to choosing the best trajectory. Eventually, it may have an impact on the engine/propeller matching calculations.

On the other hand, weather statistics may give a good overview of the probable sea conditions a ship may encounter while sailing. A thorough analysis on sea conditions may thus give a better idea of the wave added resistance over multiple trips and on the best trajectories to take.

5.2. Main project conclusions

5.2.1. Results and Discussion

The main question that was addressed was:

What method can be developed to choose the best wave added resistance model for a RoRo ship and how can statistical weather studies help optimize the performance prediction program of a wind-assisted ship?

It was then divided into two sub questions:

How can the most accurate wave added resistance model be found depending on the conditions of the case study for a RoRo ship?

and

How can statistical weather studies be used to optimize the polar matrices of a performance prediction program designed for a wind-assisted ship and reduce their size?

At the end of this research project, the proposed method to solve this first sub question was depicted and implemented. A program calculates the best model for each case study by using a decision tree made specifically for this project. All the information on the best model to choose is stored in this decision tree which was made from comparing the models and data from an existing RoRo ship. It is therefore best suited for such vessel. This extra resistance is added in a polar matrix which now takes into account the wind and wave parameters alongside with the speed and can be used by routing software made

for wind-assisted ships. This method enables to have a fast, case study adapted solution for the wave added resistance.

Furthermore, a new program was made to retrieve wind and wave data to conduct statistical weather studies and answer the second sub question. Some tests and examples showed how these studies could improve routing software designed for wind-assisted ships especially in terms of file size and computational time.

Overall, all the initial goals were met. The PyWave package works and is currently being used by the company. Moreover, TZStats was also fixed and gives consistent results with the implementation of the wave added resistance. Eventually, statistical weather studies can now be done on waves.

However, some issues arose during the research project. First of all, the lack of a formal validation of the PyWave package as it relies solely on the scientific articles and external data with large assumptions. Moreover, some assumptions had to be made on ship dimensions especially the length of run and length of entrance which are seldom mentioned. In order to remedy this first problem, the program should be compared with more reliable data to be adjusted. The positive aspect is that it is very easy to change PyWave so that the choice of the model becomes more effective.

Another issue encountered in most topics during this research project were the sizes of the files and the computational time for some programs. 6D polar matrices can quickly become quite large. In this case, a more thorough statistical analysis could find highly improbable weather conditions and remove them to simplify the matrices. The routing software's computational time tends to increase when the space step decreases. However, the space step should be as close as possible as the weather data space step will probably not be modified. Although simulating one trip does not take too long, the programs are usually used to simulate a few dozen trips hence the large computational time. In this case, parallel batch computing was mentioned to improve the computational time. For statistical studies, some attempts to improve the computational time of the data extraction have been made but were proven ineffective or even counterproductive.

5.2.2. Limits

Of course, the wave added resistance are limited by the limits of the models themselves. However, there are also new elements in this thesis. So far, it should be used for cargos equipped with WASP. The influence of the sails has not been taken into account for the wave added resistance calculation. Sails tend to create a heeling moment. It is countered by the effect of the hulls and the rudder. So far, little research has been done on this phenomenon's impact on wave added resistance [18], [44] and no semi-empirical model has been specifically designed for this type of ship. It is then quite hard to assess its influence for that matter.

It is also important to note that this project was about developing tools to provide wave added resistance values and statistical analysis rather than computing the values and analysis themselves. Thus, to this day it is complicated to evaluate if the different choice we made were relevant.

5.2.3. Suggestions for further improvements

Now that the tools have been developed, further improvements would imply a formal validation of the PyWave package especially the `model_choice_parameters2.json` in which the best models are stored for each range. This could be done with onboard data from a currently sailing RoRo ship such as Canopée for example. This operation could improve the relevance and the accuracy of the program. Perhaps a deeper study on the differences between the ship types could be considered as well.

As mentioned before, the computational time may become an issue during large scale statistical analysis. Investigating parallel computing and improving the ranges of the parameters from the occurrence

studies could be an interesting way to solve this problem.

Eventually, the size of the different files could be reduced by removing some highly improbable case scenario (high waves, low periods for example).

References

- [1] ““Wind Challenger” the Next Generation Hybrid Sailing Vessel”. In: *Third International Symposium on Marine Propulsors*. 2013.
- [2] “A Comeback of Wind Power in Shipping: An Economic and Operational Review on the Wind-Assisted Ship Propulsion Technology”. In: (2021).
- [3] “A new routing optimization tool-influence of wind and waves on fuel consumption of ships with and without wind assisted ship propulsion systems”. In: *Transportation research procedia* (2016).
- [4] “A review of wind-assisted ship propulsion for sustainable commercial shipping: latest Developments and future stakes”. In: *Wind propulsion conference*. 2021.
- [5] European Maritime Safety Agency. *Potential of wind-assisted propulsion for shipping*. Tech. rep. EMSA, 2023.
- [6] Zahra Ahmed. “Effects of Noise Pollution from Ships on Marine Life”. In: *Marine Insight* (2022).
- [7] “Analysis techniques for evaluating the fuel savings associated with wind assistance”. In: *Low Carbon Shipping conference*. 2013.
- [8] F. Pérez Arribas. “Some methods to obtain the added resistance of a ship advancing in waves”. In: *Ocean engineering* (2006).
- [9] Sverre Steen Bingjie Guo. “Added Resistance of a VLCC in Short Waves”. In: *29th International Conference on Ocean, Offshore and Arctic Engineering* (2010).
- [10] P. Boese. “Eine einfache Method zur berechnug der widerstandserhöhung eines Schiffes im see-gang”. In: (1970).
- [11] C.L.lange. “Assessing Fuel Efficiency: Hydrodynamic Design Investigation and Operational Considerations in Wind-Assisted Cruise Ships”. MA thesis. TU Delft, 2024.
- [12] Francesco Coslovich et al. “Added resistance, heave and pitch for the KVLCC2 tanker using a fully nonlinear unsteady potential flow boundary element method”. In: *Ocean engineering* (2021).
- [13] Veronika Eyring. *Brief summary of the impact of ship emissions on atmospheric composition, climate, and human health*. Tech. rep. Health and environment sub-group of the IMO, 2007.
- [14] O Faltinsen et al. “Prediction of resistance and propulsion of a ship in a Seaway”. In: *13th Symposium on Naval Hydrodynamics* (1980).
- [15] Takahashi T Fujii H. “Experimental Study on the Resistance Increase of a Large Full Ship in Regular Oblique Waves”. In: *Journal of the Society of Naval architects in Japan* (1975).
- [16] Gerritsma. “motions, wave loads and added resistance in waves of two wigley hull forms”. In: (1988).
- [17] Beukelman Gerritsma. “Analysis of the resistance increase in waves of a fast cargo ship”. In: *International shipbuilding progress* (1972).
- [18] J Gerritsma, J A Keuning, and A Versluis. “Sailing yacht performance in calm waters and waves”. In: *SNAME 11th Chesapeake sailing yacht symposium* (1993).
- [19] T.H. Havelock. “The drifting force on a ship among waves”. In: *The London, Edinburgh and Dublin philosophical magazine and journal of science* (1942).
- [20] Wellens Peter Hengelmolen Vera. “An experimental study on added resistance focused on the effects of bow wave breaking and relative wave measurements”. In: *International shipbuilding progress* (2022).
- [21] Frits Mennen Henk van den Boom Hans HUISman. “New guidelines for Speed/Power Trials level playing fiels established for IMO EEDI”. In: *Schip en werf de zee foundation* (2013).

- [22] IMO. *Interim guidelines for the calculation of the coefficient f_w for decrease in ship speed in a representative sea condition for trial use*. 2012.
- [23] Yonghwan Kim Jaehak Lee. "Development of enhanced empirical-asymptotic approach for added resistance of ships in waves". In: *Ocean engineering* (2023).
- [24] Ferdinande Jinkine. "A method for predicting the added resistance of fast cargo ships in head waves". In: *International shipbuilding progress* (1974).
- [25] Soizic Joncquez. "Second order forces and moments acting on ship in waves". PhD thesis. DTU, 2009.
- [26] Joosen. "Added resistance of ships in waves". In: *Symposium on naval hydrodynamics* (1966).
- [27] J.M.J Journée. "Experiments and Calculations on 4 Wigley Hull Forms in Head Waves". In: *Delft University of Technology Report* (1992).
- [28] Masashi Kashiwagi. "Added resistance, wave-induced steady sway force and yaw moment on an advancing ship". In: *Ship technology research* (1992).
- [29] Russel Leaper. "The Role of Slower Vessel Speeds in Reducing Greenhouse Gas Emissions, Underwater Noise and Collision Risk to Whales". In: *Sec. Marine Conservation and Sustainability* (2019).
- [30] Shukui Liu and Apostolos Papanikolaou. "Fast approach to the estimation of the added resistance of ships in head waves". In: *Ocean engineering* (2015).
- [31] Shukui Liu and Apostolos Papanikolaou. "Prediction of added resistance of ships in waves". In: *Ocean engineering* (2011).
- [32] Shukui Liu and Apostolos Papanikolaou. "Regression analysis of experimental data for added resistance in waves of arbitrary heading and development of a semi-empirical formula". In: *Ocean engineering* (2020).
- [33] Hajime Maruo. "Resistance in waves". In: *The society of Naval architects of Japan* (1963).
- [34] Hajime Maruo. "The drift of a body floating on waves". In: *Journal of Ship research* (1960).
- [35] Hajime Maruo. "The excess resistance of a ship in rough seas". In: *International shipbuilding progress* (1957).
- [36] Hajime Maruo. "Wave resistance of a ship in regular head seas". In: *Bulletin of the Faculty of engineering, Yokohama University* (1960).
- [37] No authors mentioned. *Directional wave spectra using cosine-squared and cosine 2s spreading functions*. Tech. rep. U. S. Army Engineer Waterways Experiment Station, 1985.
- [38] Malte Mitendorf et al. "Towards the uncertainty quantification of semi-empirical formulas applied to the added resistance of ships in waves of arbitrary heading". In: *Ocean engineering* (2022).
- [39] Malte Mittendorf et al. "Assessment of added resistance estimates based on monitoring data from a fleet of container vessels". In: *Ocean engineering* (2023).
- [40] Ulrik D. Nielsen et al. "Indirect Measurements of Added-Wave Resistance on an In-Service Container Ship". In: *Practical design of ships and other floating structures* (2019).
- [41] B Persson O Faltinsen K Minsaas. "On the importance of added resistance, propeller immersion and propeller ventilation for large ships in a seaway". In: *Symposium on practical design in shipbuilding* (1983).
- [42] International Maritime Organization. *Fourth IMO GHG Study 2020*. Tech. rep. International Maritime Organization, 2020.
- [43] Dong-Min Park et al. "Experimental and numerical studies on added resistance of ship in oblique sea conditions". In: *Ocean engineering* (2019).
- [44] Vinodh Pichumani. "Prediction of added resistance in waves". MA thesis. TU Delft, 2017.
- [45] "Reduced environmental impact of marine transport through speed reduction and wind assisted propulsion". In: *Transportation research* (2020).
- [46] Hamid Sadat-Hosseini et al. "CFD verification and validation of added resistance and motions of KVLCC2 with fixed and free surge in short and long head waves". In: *Ocean engineering* (2013).

- [47] Joseph Sajan. "Effect of drift angle on added resistance of a wind assisted ship". MA thesis. NTNU, 2021.
- [48] Salvensen. "Ship motions and sea loads". In: *Det Norske Veritas* (1970).
- [49] Ould el Moctar Sebastian Sigmund. "Numerical and experimental investigation of added resistance of different ship types in short and long waves". In: *Ocean engineering* (2018).
- [50] "Ship routing optimisation based on forecasted weather data and considering safety criteria". In: *The Journal of Navigation* (2022).
- [51] Shigeru NAITO Shoichi NAKAMURA. "Propulsive Performance of a Container Ship in Waves". In: *Journal of the Society of Naval architects in Japan* (1979).
- [52] Apostolos Papanikolaou Shukui Liu. "Approximation of the added resistance of ships with small draft or in ballast condition by empirical formula". In: *Journal of engineering for the maritime environment* (2017).
- [53] Jorgen strom-tejsen. "Added resistance in waves". In: *The Annual Meeting New York of The Society of Naval Architects and Marine Engineers* (1973).
- [54] Masaru Tsujimoto et al. "A practical correction method for added resistance in waves". In: *Journal of the Japan society of Naval architects and ocean engineers* (2008).
- [55] Jinbao Wang et al. "Validation study on a new semi-empirical method for the prediction of added resistance in waves of arbitrary heading in analyzing ship speed trial results". In: *Ocean engineering* (2021).
- [56] The specialist committee on Waves. *Final Report and Recommendations to the 23rd ITTC*. Tech. rep. International towing tank conference, 2002.
- [57] Ould el Moctar Wei Zhang. "Numerical prediction of wave added resistance using a Rankine Panel method". In: *Ocean engineering* (2019).
- [58] Wikipedia page, Wind wave.
- [59] Gengkun Wu. "Numerical Simulation and Backscattering Characteristics of Freak Waves Based on JONSWAP Spectrum". In: *Physical Oceanography* (2022).
- [60] Wengang Mao Xiao Lang. "A practical speed loss prediction model at arbitrary wave heading for ship voyage optimization". In: *Journal of Marine Science and Application* (2021).
- [61] Wengang Mao Xiao Lang. "A semi-empirical model for ship speed loss prediction at head sea and its validation by full-scale measurements". In: *Ocean engineering* (2020).
- [62] Sverre Steen Young-Rong Kim Ehsan Esmailian. "A meta-model for added resistance in waves". In: *Ocean engineering* (2022).